the enhanced green fluorescence protein (Adv EGFP - FZ33) prepared in FBS-free RPMI-1640 at the MOI of 1,000 vp/cell was added to each well and incubated for 1 hr at 4°C. Then the wells were washed twice with PBS and incubated at 37°C in a 5% CO_2 incubator. Twenty-four hours after infection, cells were collected and their transduction efficiencies were analyzed by flow cytometry using a FACS-Calibur®

Chemiluminescent β-Gal reporter gene assay. PC-3 cells were prepared in 96-well plates at the concentration of 5×10^3 cells/well and divided into five groups by the concentration of the mAbs and control IgG1, that is 0.001, 0.01, 0.1, 1.0, and 10 μg/ml. After removal of the culture medium, 50 μl of FBS-free RPMI-1640 at the concentrations of the mAb described above was added to each well and incubated 1 hr at 4°C. Medium was removed and microplates were washed with PBS. Fifty microliters of Adv LacZ-FZ33 at MOI of 1,000 vp/cell prepared in FBS-free RPMI-1640 was added to each well and incubated for 1 hr at 4°C. The microplates were then washed twice with PBS and incubated at 37°C in a 5% CO_2 incubator. Twenty-four hours after infection, chemiluminescent β-Gal reporter gene assays were performed. Furthermore, we compared transduction efficiency of Adv-FZ33 with wild type adenovirus (Ad5). The concentration of virus was divided into 30, 100, 300, 1,000, 3,000, and 10,000 vp/cell. The concentration of mAb and control IgG1 was 1 μg/ml.

Distribution of Target Antigens

Flow cytometric analysis. The reactivity of the mAbs with human cell lines (PC-3, LNCaP, DU145, Caki-1, T24, SKOV-3, PDF, and PrMFB) was analyzed by flow cytometry. Cells in the logarithmic growth phase were tripsinized and washed. A cell pellet containing 1×10^5 cells was suspended in staining medium (2% FBS/PBS) containing 2 μg of mAb or isotype control IgG as controls for 60 min at 4°C in the dark. After three rinses with PBS, cells were incubated with a fluorescein isothiocyanate (FITC)-conjugated rabbit anti-mouse Ig antibody (diluted 1:100) (TAGO, Inc., Burlingame, CA) for 45 min at 4°C. The cell suspension obtained was washed three times with PBS and then analyzed by flow cytometry.

Immunohistochemistry. Study specimens of 30 patients were selected from the clinical pathology archives of the Sapporo Medical University Hospital. They included 30 specimens consisting of 13 needle-core biopsies, 14 prostatectomies, and 3 cystoprostatectomies obtained between 2001 and 2002. All H&E-stained slides were reviewed and the respective diagnoses were confirmed. All of these specimens included prostatic adenocarcinoma (22 patients with Gleason scores of 5–8, and 8 with Gleason scores of 9).

Immunohistochemistry with mAbs created in this study was performed on 5-μm thick, formalin-fixed paraffin-embedded tissue sections mounted on poly L-lysine-coated slides. The concentration of the mAb as the primary antibody was 5 μg/ml. Details of immunohistochemistry methods were described in a previous study [9].

RESULTS

Establishment of Hybridomas and Mouse Monoclonal Antibodies

Cell fusions done three times produced hybridoma colonies in 2,500 wells. We cloned the hybridomas from wells with high β-Gal activity by limiting dilution, because the β-Gal activity of each well reflected the transfection efficiency into PC-3 cells via the antigen recognized by the antibodies secreted from the hybridoma. We thereby established hybridomas secreting mAb 1B7, 2H7, 6F8, and 9B10. Isotypes of mAb 1B7, 2H7, and 6F8 were determined to be IgG1 kappa and, for mAb 9B10, IgG2a kappa.

Identification of mAbs 1B7, 2H7, 6F8, and 9B10 Antigens

Biotinylated proteins were detected at 40 kDa by immunoprecipitation using mAb 1B7 (Fig. 2A). Silver stain detected the same proteins. The epithelial cell adhesion molecule (Ep-CAM) was detected by mass spectrometry (Fig. 2B,C). cDNA of Ep-CAM was transfected into 293 T cells. Flow cytometry revealed that mAb 1B7 reacted with transfectants expressing Ep-CAM (Fig. 2D). We therefore concluded that the antigen recognized by mAb 1B7 was Ep-CAM.

In immunoprecipitation using mAb 2H7, an 80 kDa protein was detected (Fig. 3A). The protein was identified as poliovirus receptor (CD155) by mass spectrometry (Fig. 3B,C). cDNA of human CD155 was transfected into CHO cells and mAb 2H7 reacted with cells expressing CD155 (Fig. 3D).

In immunoprecipitation using mAb 6F8, 110, and 50 kDa biotinylated proteins were detected (Fig. 4A). The 110 kDa silver-stained protein, which was sharper than the 50 kDa band, was extracted and analyzed by mass spectrometry (Fig. 4B,C). The protein was identified as Na,K-ATPase β1. We obtained the cDNAs of human Na,K-ATPase α1, Na,K-ATPase α2, Na, K-ATPase α3, Na,K-ATPase α4 transcript variant 2, Na, K-ATPase β1, Na,K-ATPase β2, and Na,K-ATPase β3 to determine the antigens. Each cDNA was transfected into CHO cells and it was found that mAb6F8 reacted

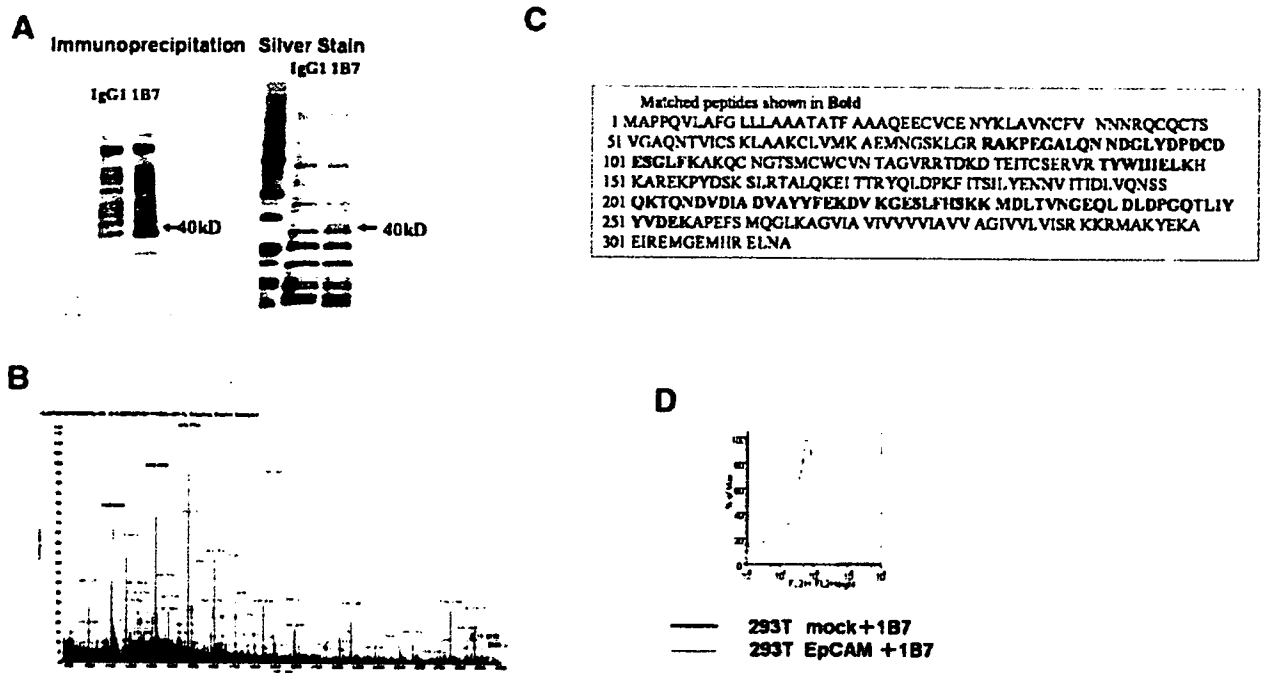

Fig. 2. Identification of mAb 1B7 antigen. **A**: Lysates of PC-3 cells were immunoprecipitated with mAb 1B7; proteins (40 kDa) were detected. The band that appeared at 40 kDa (indicated by an arrow) was excised from the gel and analyzed by mass spectrometry. **B**: High-intensity spectra indicated by a rectangles indicate the peptide, the sequence of which corresponded to the amino acid sequence of human Ep-CAM. **C**: Boldface indicates the sequence of the detected peptide. **D**: Flow cytometry of the reactivity of mAb 1B7 with 293T cells transfected with cDNA of Ep-CAM. mAb 1B7 reacted only with 293T cells transfected with cDNA of Ep-CAM.

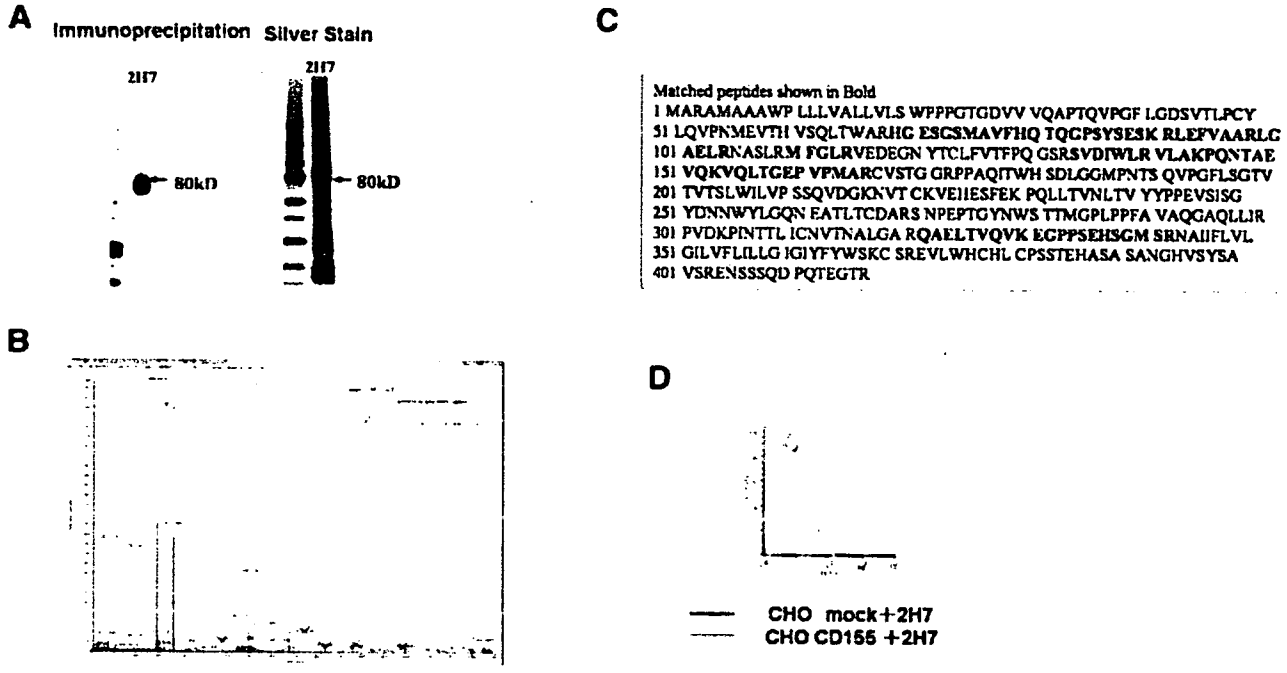

Fig. 3. Identification of mAb 2H7 antigen. **A**: Immunoprecipitation with mAb 2H7. The band that appeared at 80 kDa (indicated by an arrow) was excised from the gel and analyzed by mass spectrometry. **B**: Encircled high-intensity spectra indicate the peptide, the sequence of which corresponded to the amino acid sequence of human CD155. **C**: Boldface indicates the sequence of the detected peptide. **D**: Flow cytometry of the reactivity of mAb 2H7 with CHO cells transfected with cDNA of CD155. mAb 2H7 reacted only with CHO cells transfected with cDNA of CD155.

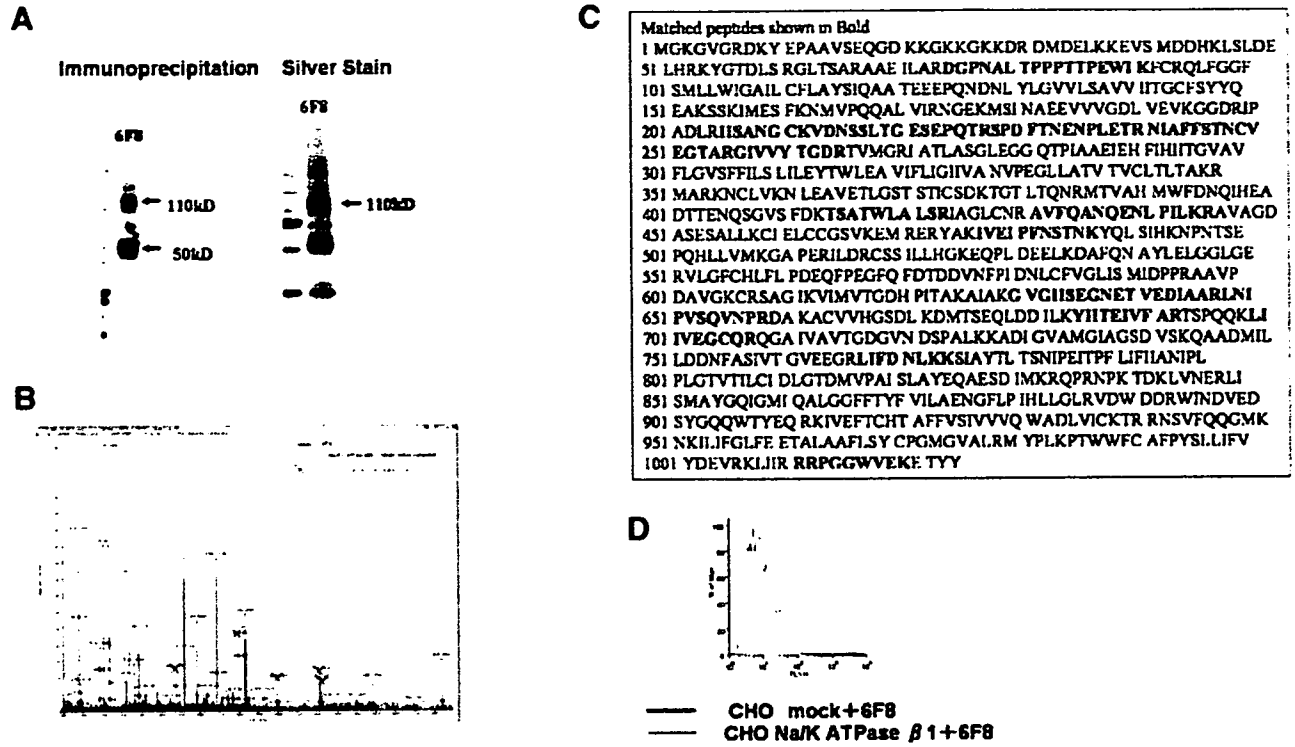

Fig. 4. Identification of mAb 6F8 antigen. **A**: immunoprecipitation with mAb 6F8; proteins (110 and 50 kDa) were detected. The band that appeared at 110 kDa was excised from the gel and analyzed by mass spectrometry. **B**: Encircled high-intensity spectra indicate the peptide, the sequence of which corresponded to the amino acid sequence of human Na,K-ATPase αI. **C**: Boldface indicates the sequence of the detected peptide. **D**: Flow cytometry of the reactivity of mAb 6F8 with CHO cells transfected with the cDNA of each subunit and isozyme of human Na,K-ATPase. mAb 6F8 reacted only with CHO cells transfected with cDNA of human Na,K-ATPase βI.

only with the transfectant expressing the Na,K-ATPase β1 subunit (Fig. 4D). We therefore concluded that the antigen recognized by mAb 6E3 was Na,K-ATPase β1.

In immunoprecipitation using mAb 9B10, a 55 kDa protein was detected (Fig. 5A). The protein was identified as HAI-1 by mass spectrometry (Fig. 5B,C). cDNA of human hepatocyte growth factor activator inhibitor type 1 (HAI-1) transcript variant 2 and HAI-1 transcript variant 3 were obtained. Each cDNA was transfected into CHO cells. mAb 9B10 reacted with each transfectant (Fig. 5D). Therefore, we concluded that mAb 9B10 recognized HAI-1.

Transfection Efficiency Into PC-3 With mAbs and Adv-FZ33

Flow cytometric analysis. Transfection efficiency was evaluated with various mAbs. Cells transfected using AdvEGFP-FZ33 together with mAb 1B7, 2H7, 6F8, and 9B10 showed enhanced expression EGFP compared with those together with mouse IgG1 (Fig. 6A).

Chemiluminescent β-Gal reporter gene assay. β-Gal activity in mAb 1B7, 2H7, and 6F8 at the concentration 1.0 μg/ml showed about 70-fold enhancement compared with control mouse IgG1. In mAb 9B10, transfection efficiency showed about 10-fold enhancement (Fig. 6B). Adv LacZ-FZ33 with mAb 6F8 showed significantly high expression of β-Gal compared with wild type—fiber adenovirus with or without mAb (Fig. 6C).

Distribution of Target Antigens

Expression in several cell lines. We examined the reactivities of mAb 1B7, 2H7, 6F8, and 9B10 with cancer and non-cancer cell lines by flow cytometry. mAb 2H7 and 6F8 reacted strongly with all cell lines (Fig. 7B,C). mAb 1B7 reacted with all cancer cell lines but not with PrMFB and PDF (Fig. 7A). mAb 9B10 did not react with SKOV-3, PrMFB, or PDF (Fig. 7D).

Histologic findings on the specimens. All of the prostate cancer cells (Fig. 8A,C) and most of the normal epithelial cells (Fig. 8B) showed strong immunoreactivity for mAb 1B7 in all the samples. Some of the normal epithelial cells (Fig. 8C,D) and all of the stromal cells (Fig. 8A–D) showed negative staining. No samples were stained with the other three mAbs.

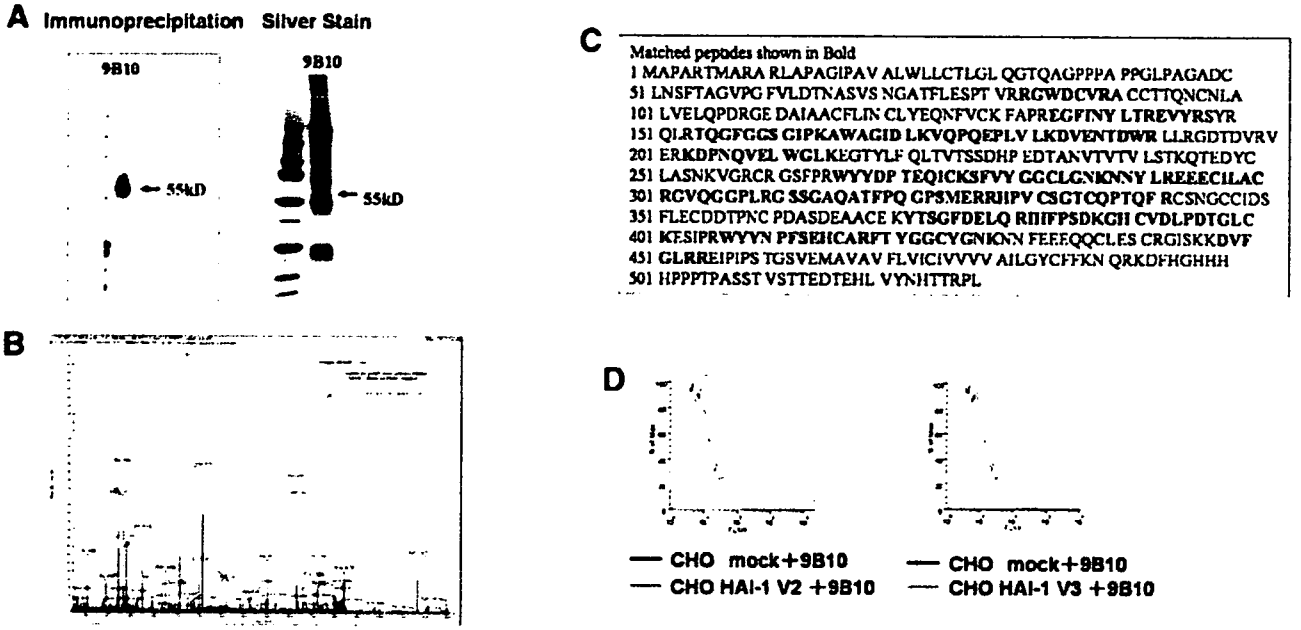

Fig. 5. Identification of mAb 9B10 antigen. **A**: immunoprecipitation with mAb 9B10. The band that appeared at 55 kDa (indicated by an arrow) was excised from the gel and analyzed by mass spectrometry. **B**: Encircled high-intensity spectra circle indicate the peptide, the sequence of which corresponded to the amino acid sequence of human HAI-1. **C**: Boldface indicates the sequence of the detected peptide. **D**: Flow cytometry of the reactivity of mAb 9B10 with CHO cells transfected with cDNA of each subunit of HAI-1. mAb9B10 reacted with CHO cells transfected with cDNA of each subunit of HAI-1.

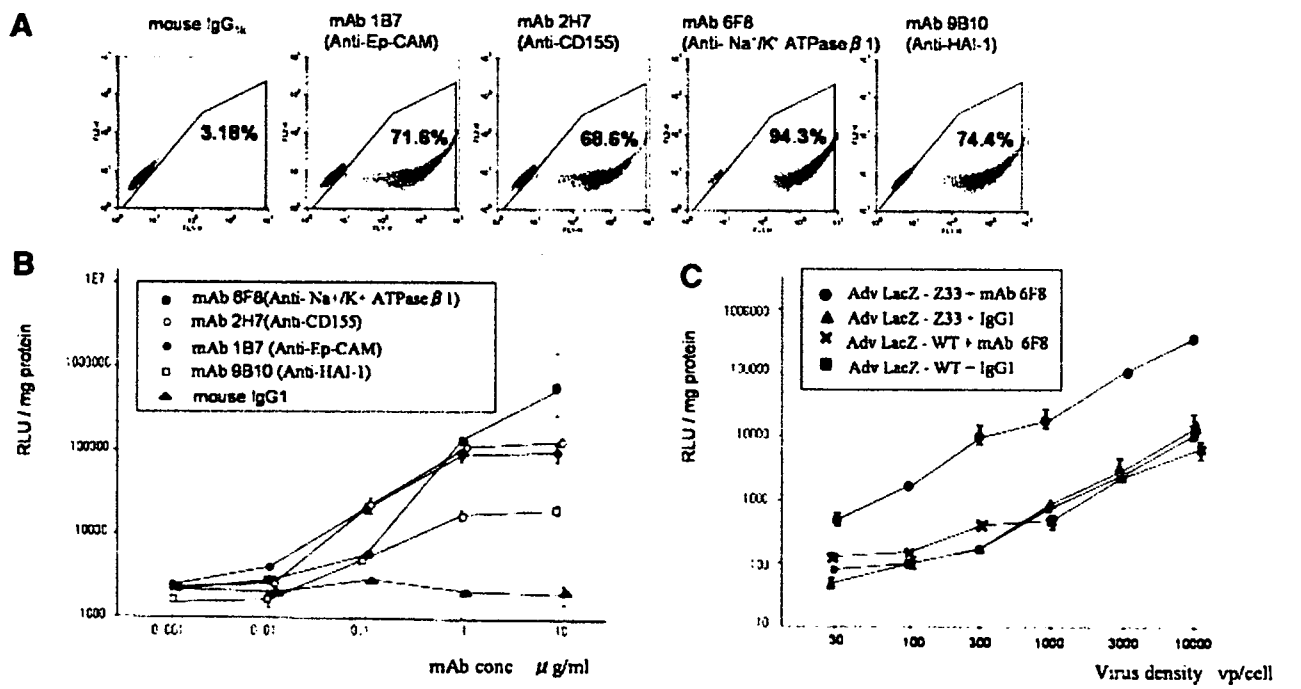

Fig. 6. Transfection efficiency into PC-3 cells with each fiber mutant adenovirus-mediated mAb. **A**: Numbers presented in each panel indicate the percentage of cells expressing EGFP. Cells transfected using AdvEGFP-FZ33 together with mIgGI showed low expression of EGFP. Cells transfected using AdvEGFP-FZ33 together with mAbs 1B7(anti-Ep-CAM mAb), 2H7(anti-CD155 mAb), 6F8(Na,K-ATPase βI mAb), and 9B10(anti-HAI-1 mAb) showed enhanced expression of EGFP. **B**: The cells were lysed, and assayed for β-Gal activity using a commercial kit (n = 4). AdvEGFP-FZ33 together with mAbs 1B7, 2H7, 6F8, and 9B10 showed high transduction efficiency compare with control IgG. **C**: Adv LacZ - FZ33 together with mAb 6F8 showed high transduction efficiency compared with wild type adenovirus (Adv Lacz–WT).

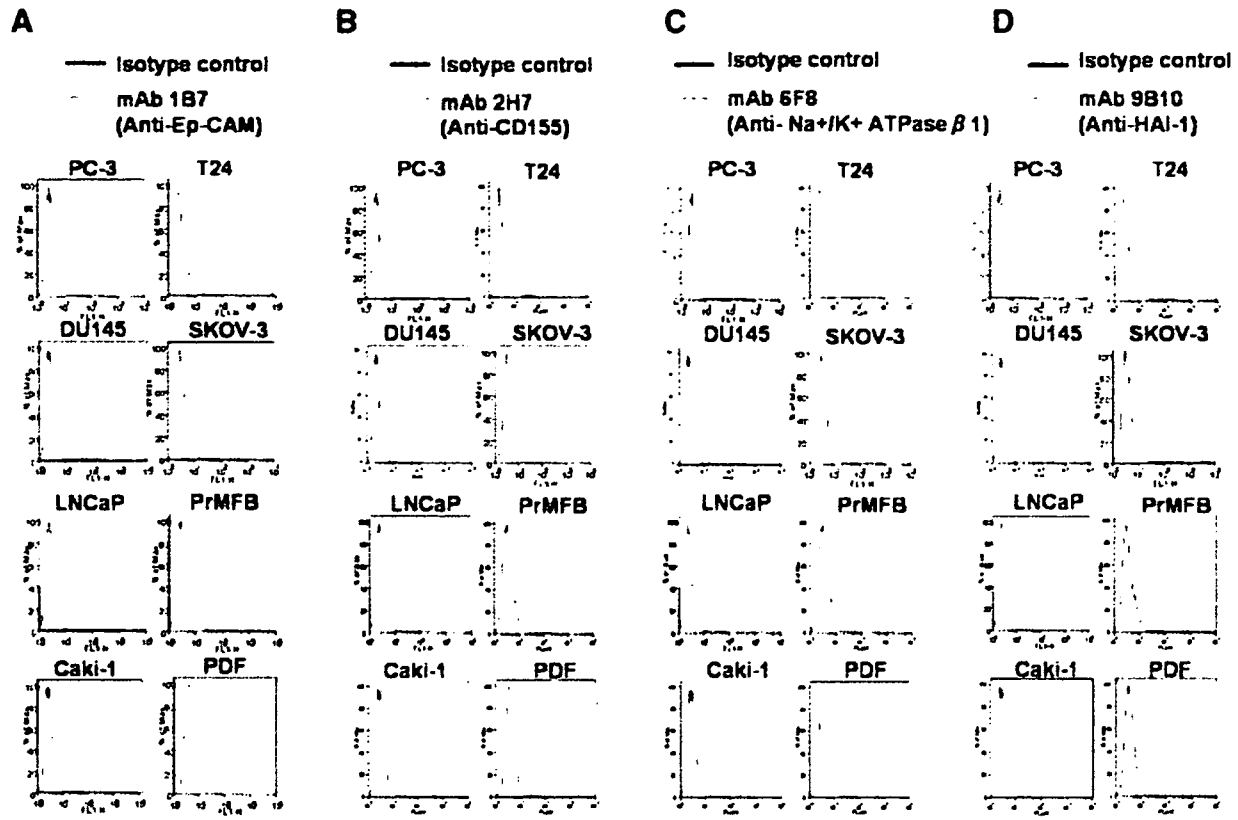

Fig. 7. Reactivities of established mAbs with various human cell lines. **A**: Antigen of mAb 1B7 was expressed on the surface of PC-3, DU145, LNCaP, Caki-1, T24, and SKOV-3 but not PrMFB and PDF. **B,C**: Antigens of mAbs 1B7 and 6F8 were expressed on the surface of each cell line. **D**: Antigen of mAb 9B10 was expressed on the surface of PC-3, DU145, LNCaP, Caki-1, and T24 but not SKOV-3, PrMFB, or PDF.

DISCUSSION

Volspers et al. [6] constructed a Z33-modified adenovirus vector and reported that the transduction efficiency of this modified vector in epidermal growth factor receptor (EGFR)-expressing cells was strongly and dose-dependently enhanced by combination with an EGFR-specific monoclonal antibody. They suggested that antibody-mediated targeting of the Z33-modified adenovirus vector could be applied for directed gene transfer to a wide variety of cell types by simply changing the target-specific antibody. Tanaka et al. [8] evaluated, both in vitro and in vivo, the extent of retargeting toward and therapeutic effectiveness against carcinoembryonic antigen (CEA)-positive gastric cancers when using the fully human CEA antibody complex with Adv-FZ33. They generated Ax3CAUP-FZ33 (UP-FZ33), an Adv-FZ33 derivative vector expressing a therapeutic gene (*Escherichia coli* uracil phosphoribosyltransferase) that converted 5-fluorouracil (5-FU) directly to 5-fluoro-UMP. UP-FZ33 with the anti-CEA mAb enhanced the cytotoxicity of 5-FU by 10.5-fold in terms of the IC_{50} against a CEA-positive gastric cancer cell line compared with control IgG4. In a nude mouse peritoneal dissemination model, tumor growth in mice treated by UP-FZ33 premixed with the anti-CEA mAb was significantly suppressed, and the median survival time was significantly longer than in the control group.

Surface antigens may be a viable target for antibody-mediated gene therapy. Although, PSA is a clinically important biomarker in prostate cancer [10,11], PSA is not a surface antigen [12]. Although, prostate-specific membrane antigen (PSMA) [13] is a type II membrane antigen, the PSMA expression pattern is not fully restricted to the prostate [14,15]. Therefore, we investigated target molecules amenable to gene therapy with Adv-FZ33. In this study, we immunized mice with three human cell lines that were androgen-independent (PC-3 and DU145) or androgen-dependent (LNCaP) [16], for generating various types of mouse mAbs. We have performed to screening the target antibodies using human prostate cancer cell line PC-3. Although, our Adv-FZ33 has intact CAR-binding structure and retains CAR-binding ability, CAR protein is downregulated in the highly tumorigenic PC-3 cell line [17] and the transduction efficiency of adenovirus is quit low (Fig. 6). Furthermore, PC-3 does

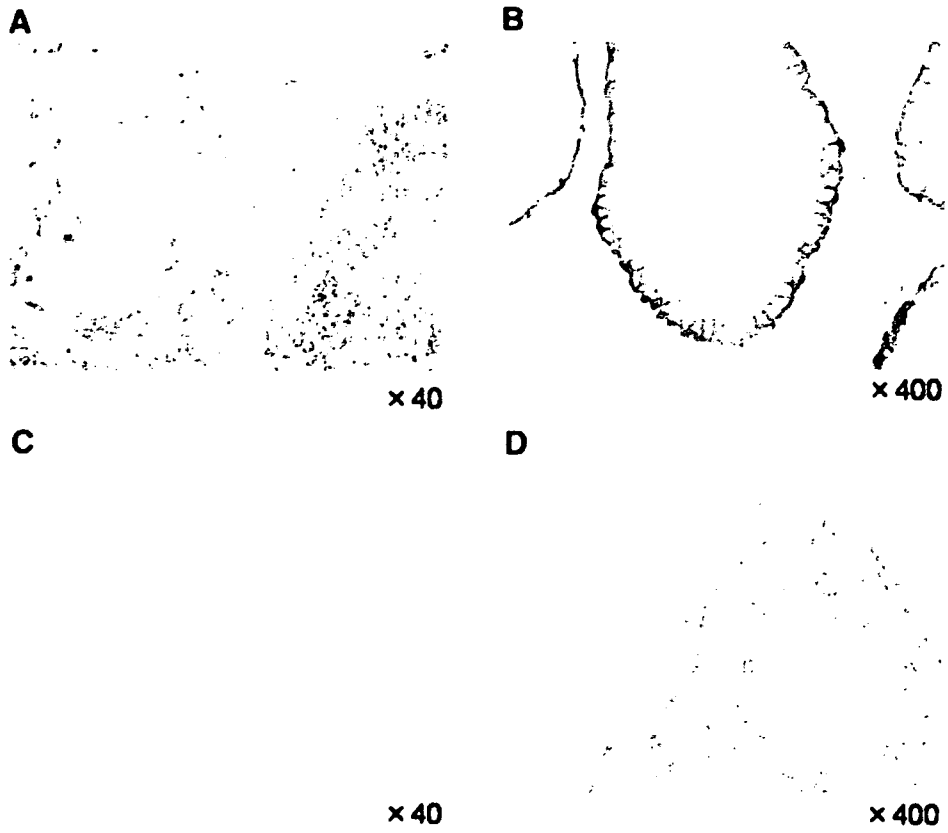

Fig. 8. Immunohistochemical findings for prostate cancer cells and normal epithelial cells of the prostate. **A**: Prostate cancer and normal epithelial cells shows strong immunoreactivity for mAb 1B7. **B**: Basolateral cell surface of normal epithelium shows strong immunoreactivity for mAb 1B7. **C**: Prostate cancer shows strong immunoreactivity for mAb 1B7 but normal epithelial cells do not. **D**: Normal epithelial cells are not stained. Stromal cells are not stained in each sample.

not express PSMA. The first aim of this study is to target adenovirus to resistant cell line PC-3.

We purified four different mAbs and confirmed high transduction efficiency by flow cytometry and chemiluminescent β-Gal reporter gene assay. The target molecules of mAbs 1B7, 2H7, 6F8, and 9B10 were Ep-CAM, CD155, Na,K-ATPase β1, and HAI-1, respectively. CD155 and Na,K-ATPase β1 found to be widely expressed by flow cytometric analysis are inappropriate molecules for tumor targeting. The anti-Ep-CAM antibody mAb 1B7 and anti-HAI-1 antibody mAb 2H7 showed reactivity with cancer cell lines other than fibroblast cell lines. We could not find reactivity with prostate cancer samples for mAb 2H7, 6F8, or 9B10. These mAbs may be unsuitable for staining of samples fixed in formalin. In mAb 1B7, we found that Ep-CAM expression on prostate cancer cells was stronger than on normal epithelial cells, but not significantly. In 1979, Ep-CAM was discovered in a search for novel cell surface antigens expressed on neoplastic tissue [18]. Ep-CAM is known to be expressed on the basolateral cell surfaces of selected normal epithelia and many carcinomas [19–22]. Of particular interest, overexpression of Ep-CAM has been reported in prostate cancer [21,23]. Clinical trials of mAbs directed against Ep-CAM for immunologic therapy have been conducted in patients with colon cancer [24]. Recently, clinical phase I study with anti-Ep-CAM humanized IgG1 have been performed in patients with hormone refractory prostate cancer by Oberneder et al. [25]. Heideman et al. [26] showed that Ep-CAM targeted vectors using bispecific antibodies against the adenovirus fiber-knob protein, and Ep-CAM may be useful for gastric and esophageal cancer-specific gene therapy. HAI-1 is a novel Kunitz-type serine protease inhibitor first reported in 1997 [27]. Although, HAI-1 is broadly expressed in epithelial cells of most human tissues [28,29], Knudsen et al. [30] reported that its expression was significantly increased in localized prostate cancer and was present in most prostate cancer metastases compared to normal prostate glands. Furthermore, HAI-1 overexpression in prostate cancer was predictive of prostate-specific antigen recurrence. Nagakawa et al. [31] demonstrated that significantly increased serum levels of HAI-1 were detected in patients with prostate cancer, indicating that HAI-1

would be a potential tumor marker for prostate cancer. Ep-CAM and HAI-1 overexpressed in prostate cancer may be potential targets for prostate cancer gene therapy with Adv-FZ33, although therapeutic effectiveness must be evaluated as well. In future clinical application, we would like to use Adv-FZ33 premixed with prostate cancer targeting mAb prior to injection. This method seems to be more practical for administration systemically.

In addition to mAb 1B7 and 9B10, we may be able to establish new prostate cancer-specific mAbs through the hybridoma screening system that was designed in this study. Previously, Lampe et al. [32] performed fusions 25 times and developed three mAb directed against prostate associated antigens that might identify potential new therapeutic targets through screening of circa 25,000–50,000 hybridomas. We evaluated only 2,500 wells through three fusions and identified potential four target molecules. Overall, this approach of inductive method using FZ33 fiber-modified adenovirus is reliable strategy for screening useful mAbs that recognize target molecules in prostate cancer gene therapy as well as antibody therapy and diagnosis.

CONCLUSIONS

We established hybridoma from mice immunized with prostate cancer cell lines and selected anti-Ep-CAM mAb and anti-HAI-1 mAbs. Using Adv-FZ33, these mAbs increased transduction efficiency to prostate cancer cells. Gene transduction via Ep-CAM and HAI-1 may be a novel strategy for treatment of prostate cancer.

ACKNOWLEDGMENTS

The authors thank Ms. Toshie Kurohata for her technical assistance. This study was partly supported by the Stiftelsen Japanese-Swedish Cooperative Foundation (T. Tsukamoto), by Grant-in-Aid for Cancer Research from the Ministry of Health and Welfare of Japan (K. Kato and H. Hamada) and by Grant-in-Aid for Scientific Research on Priority Areas "Cancer" from the Ministry of Education, Culture, Sports, Science and Technology (K. Kato, K. Nakamura, and H. Hamada).

REFERENCES

1. Jemal A, Thomas A, Murray T, Thun M. Cancer statistics. CA Cancer J Clin 2002;52:23–47.
2. Kasper S, Cookson MS. Mechanism leading to the development of hormone-resistant prostate cancer. Urol Clin N Am 2006;33: 201–210.
3. Macrae EJ, Giannoudis A, Ryan R, Brown NJ, Hamdy FC, Maitland N, Lewis CE. Gene therapy for prostate cancer: Current strategies and new cell-based approaches. Prostate 2006;66:470–494.
4. Brody SL, Crystal RG. Adenovirus-mediated in vivo gene transfer. Ann N Y Acad Sci 1994;716:90–101; (discussion 101–103).
5. Bergelson JM, Cunningham JA, Droguett G, Kurt-Jones EA, Krithivas A, Hong JS, Horwitz MS, Crowell RL, Finberg RW. Isolation of a common receptor for Coxsackie B viruses and adenoviruses 2 and 5. Science 1997;275:1320–1323.
6. Volpers C, Thirion C, Biermann V, Hussmann S, Kewes H, Dunant P, von der Mark H, Herrmann A, Kochanek S, Lochmuller H. Antibody-mediated targeting of an adenovirus vector modified to contain a synthetic immunoglobulin g-binding domain in the capsid. J Virol 2003;77:2093–2104.
7. Hisataki T, Itoh N, Suzuki K, Takahashi A, Masumori N, Tohse N, Ohmori Y, Yamada S, Tsukamoto T. Modulation of phenotype of human prostatic stromal cells by transforming growth factor-betas. Prostate 2004;58:174–182.
8. Tanaka T, Huang J, Hirai S, Kuroki M, Kuroki M, Watanabe N, Tomihara K, Kato K, Hamada H. Carcinoembryonic antigen-targeted selective gene therapy for gastric cancer through FZ33 fiber-modified adenovirus vectors. Clin Cancer Res 2006;12: 3803–3813.
9. Kitamura H, Torigoe T, Asanuma H, Hisasue SI, Suzuki K, Tsukamoto T, Satoh M, Sato N. Cytosolic overexpression of p62 sequestosome 1 in neoplastic prostate tissue. Histopathology 2006;48:157–161.
10. Getzenberg RH, Abrahamsson PA, Canto EI, Chinnaiyan AM, Djavan B, Laxman B, Ogawa O, Slawin K, Tomlins SA, Yu J. Advances in biomarkers for prostatic disease. In: McConnell J, Denis L, Akaza H, Khoury S, Schalken J, editors. Prostate Cancer. Paris: Health Publications; 2006. pp 85–148.
11. Lieberman R. Evidence-based medical perspectives: The evolving role of PSA for early detection, monitoring of treatment response, and as a surrogate end point of efficacy for interventions in men with different clinical risk states for the prevention and progression of prostate cancer. Am J Ther 2004;11:501–506.
12. Migita T, Oda Y, Naito S, Morikawa W, Kuwano M, Tsuneyoshi M. The accumulation of angiostatin-like fragments in human prostate carcinoma. Clin Cancer Res 2001;7:2750–2756.
13. Horoszewicz JS, Kawinski E, Murphy GP. Monoclonal antibodies to a new antigenic marker in epithelial prostatic cells and serum of prostatic cancer patients. Anticancer Res 1987;7:927–935.
14. Israeli RS, Powell CT, Corr JG, Fair WR, Heston WD. Expression of the prostate-specific membrane antigen. Cancer Res 1994;54: 1807–1811.
15. Sokoloff RL, Norton KC, Gasior CL, Marker KM, Grauer LS. A dual-monoclonal sandwich assay for prostate-specific membrane antigen: Levels in tissues, seminal fluid and urine. Prostate 2000;43:150–157.
16. Janssen T, Darro F, Petein M, Raviv G, Pasteels JL, Kiss R, Schulman CC. In vitro characterization of prolactin-induced effects on proliferation in the neoplastic LNCaP, DU145, and PC-3 models of the human prostate. Cancer 1996;77:144–149.
17. Okegawa T, Li Y, Pong RC, Bergelson JM, Zhou J, Hsieh JT. The dual impact of coxsackie and adenovirus receptor expression on human prostate cancer gene therapy. Cancer Res 2000;60:5031–5036.
18. Herlyn M, Steplewski Z, Herlyn D, Koprowski H. Colorectal carcinoma-specific antigen: Detection by means of monoclonal antibodies. Proc Natl Acad Sci USA 1979;76:1438–1442.
19. Momburg F, Moldenhauer G, Hammerling GJ, Moller P. Immunohistochemical study of the expression of a Mr 34,000

human epithelium-specific surface glycoprotein in normal and malignant tissues. Cancer Res 1987;47:2883–2891.

20. Xie X, Wang CY, Cao YX, Wang W, Zhuang R, Chen LH, Dang NN, Fang L, Jin BQ. Expression pattern of epithelial cell adhesion molecule on normal and malignant colon tissues. World J Gastroenterol 2005;11:344–347.
21. Went P, Vasei M, Bubendorf L, Terracciano L, Tornillo L, Riede U, Kononen J, Simon R, Sauter G, Baeuerle PA. Frequent high-level expression of the immunotherapeutic target Ep-CAM in colon, stomach, prostate and lung cancers. Br J Cancer 2006;94: 128–135.
22. Heinzelmann-Schwarz VA, Gardiner-Garden M, Henshall SM, Scurry J, Scolyer RA, Davies MJ, Heinzelmann M, Kalish LH, Bali A, Kench JG, Edwards LS, Vanden Bergh PM, Hacker NF, Sutherland RL, O'Brien PM. Overexpression of the cell adhesion molecules DDR1, claudin 3, and Ep-CAM in metaplastic ovarian epithelium and ovarian cancer. Clin Cancer Res 2004;10:4427–4436.
23. Poczatek RB, Myers RB, Manne U, Oelschlager DK, Weiss HL, Bostwick DG, Grizzle WE. Ep-Cam levels in prostatic adenocarcinoma and prostatic intraepithelial neoplasia. J Urol 1999; 162:1462–1466.
24. Mosolits S, Nilsson B, Mellstedt H. Towards therapeutic vaccines for colorectal carcinoma: A review of clinical trials. Expert Rev Vaccines 2005;4:329–350.
25. Oberneder R, Weckermann D, Ebner B, Quadt C, Kirchinger P, Raum T, Locher M, Prang N, Baeuerle PA, Leo E. A phase I study with adecatumumab, a human antibody directed against epithelial cell adhesion molecule, in hormone refractory prostate cancer patients. Eur J Cancer 2006;42:2530–2538.
26. Heideman DA, Snijders PJ, Craanen ME, Bloemena E, Meijer CJ, Meuwissen SG, van Beusechem VW, Pinedo HM, Curiel DT, Haisma HJ, Gerritsen WR. Selective gene delivery toward gastric and esophageal adenocarcinoma cells via EpCAM-targeted adenoviral vectors. Cancer Gene Ther 2001;8:342–351.
27. Shimomura T, Denda K, Kitamura A, Kawaguchi T, Kito M, Kondo J, Kagaya S, Qin L, Takata H, Miyazawa K, Kitamura N. Hepatocyte growth factor activator inhibitor, a novel Kunitz-type serine protease inhibitor. J Biol Chem 1997;272:6370–6376.
28. Kataoka H, Suganuma T, Shimomura T, Itoh H, Kitamura N, Nabeshima K, Koono M. Distribution of hepatocyte growth factor activator inhibitor type 1 (HAI-1) in human tissues. Cellular surface localization of HAI-1 in simple columnar epithelium and its modulated expression in injured and regenerative tissues. J Histochem Cytochem 1999;47:673–682.
29. Oberst M, Anders J, Xie B, Singh B, Ossandon M, Johnson M, Dickson RB, Lin CY. Matriptase and HAI-1 are expressed by normal and malignant epithelial cells in vitro and in vivo. Am J Pathol 2001;158:1301–1311.
30. Knudsen BS, Lucas JM, Fazli L, Hawley S, Falcon S, Coleman IM, Martin DB, Xu C, True LD, Gleave ME, Nelson PS, Ayala GE. Regulation of hepatocyte activator inhibitor-1 expression by androgen and oncogenic transformation in the prostate. Am J Pathol 2005;167:255–266.
31. Nagakawa O, Yamagishi T, Akashi T, Nagaike K, Fuse H. Serum hepatocyte growth factor activator inhibitor type I (HAI-I) and type 2 (HAI-2) in prostate cancer. Prostate 2006;66:447–452.
32. Lampe MI, Molkenboer-Kuenen JD, Oosterwijk E. Development of new prostate specific monoclonal antibodies. Prostate 2004; 58:225–231.

Gene Therapy (2008) 15, 203–213

www.nature.com/gt

ORIGINAL ARTICLE

Gene transfer of CD40-ligand to dendritic cells stimulates interferon-γ production to induce growth arrest and apoptosis of tumor cells

K Tomihara[1,2], K Kato[1], Y Masuta[1], K Nakamura[1], H Uchida[1], K Sasaki[1], T Tanaka[1], J Huang[1], H Hiratsuka[2] and H Hamada[1]

[1]Department of Molecular Medicine, Sapporo Medical University, Sapporo, Japan and [2]Department of Oral Surgery, Sapporo Medical University, Sapporo, Japan

In this study, we present evidence that gene transfer of the CD40-ligand (CD154) into human immature dendritic cells (DC) imparts direct antitumor effects on tumor cells. DC infected with adenovirus directed to express human CD154 on the cell surface (CD154-DC) elicited significantly higher levels of immune accessory molecules commonly found on mature DC. We found that co-cultivation with a human squamous cell carcinoma cell line (OSC-70) with CD154-DC significantly inhibited cell growth. We further demonstrate that OSC-70 cells stimulated with CD154-DC were more susceptible to apoptosis via TNF-related apoptosis inducing ligand (TRAIL). Importantly, tumor cells co-cultured with CD154-DC in transwell plates expressed upregulated cell surface TRAIL-R2. CD154-DC produced higher levels of interferon (IFN)-γ, IL-12p70 and soluble CD154, but the ability of CD154-DC to inhibit tumor cell growth was significantly abrogated by a neutralizing antibody to IFN-γ, indicating that this was mainly mediated by IFN-γ. Furthermore, intratumoral injection of CD154-DC significantly suppressed OSC-70 tumor growth in a xenograft model. Overall, these results reveal that CD154-DC have potential as an anti-cancer therapy by producing IFN-γ to arrest adjacent tumor cell growth and increase the susceptibility of apoptosis via TRAIL.
Gene Therapy (2008) 15, 203–213; doi:10.1038/sj.gt.3303056; published online 8 November 2007

Keywords: *CD40-ligand; adenoviral vector; dendritic cells; immune gene therapy; IFN-γ; TRAIL*

Introduction

Dendritic cells (DC) are the most potent of antigen presenting cells and play a central role in the induction of the innate immune response. It is well known that DC show an important role for tumor elimination followed by the activation of cytotoxic T cells (CTL).[1] In addition to the generation of tumor-specific CTL, recent studies have shown that DC have a direct antitumor effect and activate the innate immune system. In one report, human monocytes and DC stimulated with interferon (IFN)-α or IFN-γ produced cytotoxic effects on tumor cells through the TRAIL pathway.[2,3] Another study demonstrated that human monocyte-derived DC stimulated with CD154 induced tumor necrosis factor (TNF)-α production that, in part, mediated the cytotoxic effects on tumor cells.[4] Finally, it was reported that IFN-γ-stimulated DC or soluble factors secreted from lipopolysaccharide (LPS)-stimulated DC inhibited tumor cell growth.[5] While much evidence clearly defines an important role for DC in eliminating tumor cells, the mechanisms behind these direct antitumor effects are not entirely clear.

Correspondence: Dr K Kato, Department of Molecular Medicine, Sapporo Medical University, South 1, West 17, Chuo-ku, Sapporo 060-8556, Japan.
E-mail: kakazu@sapmed.ac.jp
Received 28 March 2006; revised 3 May 2007; accepted 10 June 2007; published online 8 November 2007

Activation of DC for the subsequent induction of antigen-specific T-cell responses and cytokine production requires CD40 ligation. However, DC in various maturation stages can produce cytokines in response to different stimuli. CD154-stimulated DC can secrete high amounts of interleukin-12 (IL-12), which is essential for the activation of T cells and natural killer (NK) cells by DC.[6] Precursor DC have the ability to produce type 1 IFNs,[7,8] and those activated by viral infection can produce higher amounts that activate NK cells and macrophages. Further, murine macrophages and lymphoid DC stimulated with IL-12 or IL-18 have been shown to produce IFN-γ.[9–12] While IFN-γ can regulate some apoptotic events and was shown recently to be a major modulator of death inducing stimuli such as TRAIL, there are no reports that CD154-stimulated DC can produce IFNs.

In the present study, we evaluated the antitumor effects of DCs transduced with the human CD154 gene (CD154-DC) on a co-cultured human squamous cell carcinoma cell line, OSC-70. In both mixed co-cultures and transwell co-cultures, tumor cell growth was suppressed. Further, cell death was induced strongly by TRAIL without direct contact by CD154-DC. We have demonstrated that significantly higher amounts of IFN-γ were produced in culture supernatants of CD154-DC, and it was critical factor for CD154-DC-mediated tumor growth suppression. Consequently, antitumor therapeutic potential of CD154-DC was investigated.

Results

Phenotypic alterations of dendritic cells transduced with CD154

Adenovirus-infected DC were evaluated for the expression of various DC-lymphocyte co-stimulatory molecules by flow cytometry and by morphologic changes via photomicroscopy. In contrast to immature DC (im-DC) or DC transduced with *lacZ* (LacZ-DC), DC transduced with CD154 (CD154-DC) expressed high levels of CD154 as a transgene following CD80, CD83 and CD86 as DC maturation/activation markers (Figure 1a). CD154-DC strongly attached to the culture dish and were altered in morphology with respect to spindle shape and dendritic shape (Figure 1b). These data indicate that adenovirus encoding human CD154 is effective in inducing DC maturation and activation.

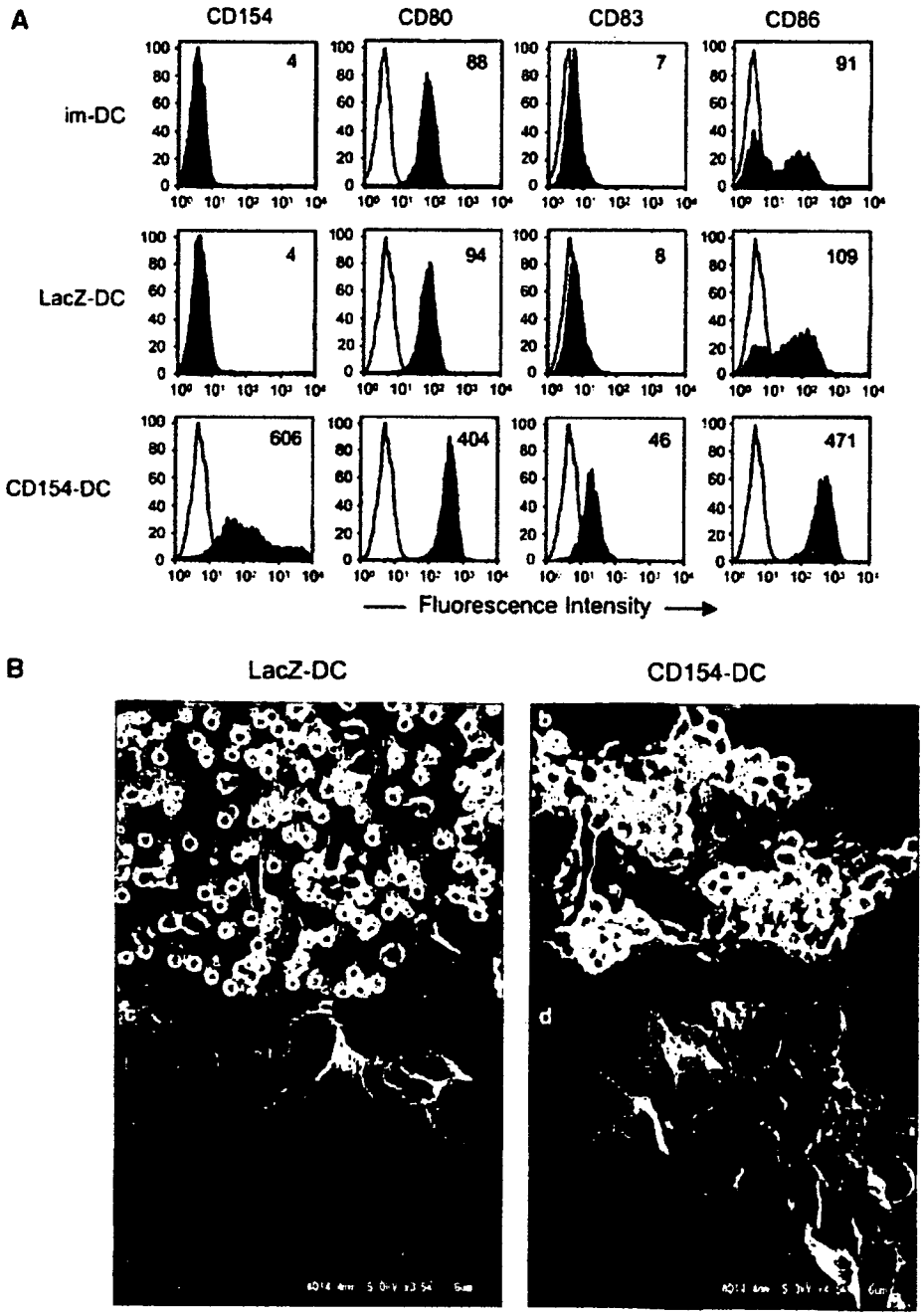

Figure 1 Phenotypic and morphologic changes of human dendritic cells (DC) infected with Adv-CD154. Immature dendritic cells derived from PBMC from a healthy donor were infected with either AxCAhCD154-F/RGD or AxCAZ3-F/RGD (control vector). (A) Surface expression of CD154, CD80, CD83 and CD86 on dendritic cells 48 h post-adenovirus infection by flow cytometry. Open histograms represent staining with anti-human IgG negative control mAb. Oblique-lined histograms represent staining with FITC-or PE-conjugated specific mAb, respectively. The number in each panel represents the mean fluorescence intensity ratio. One of data in three independent experiments was represented. (B) Optical (a, b) and electron (c, d) photomicrographs of dendritic cells 48 h post-adenovirus encoding LacZ (*left*) or CD154 (*right*) infection.

CD154-DC suppressed the tumor cell growth

To investigate whether CD154-DC exhibited direct antitumor effects, we assessed the growth of co-cultured human oral squamous cell carcinoma, OSC-70 cells. OSC-70 cells were co-cultured with CD154-DC at several DC vs tumor cell ratios. As controls, OSC-70 cells were also co-cultured with LacZ-DC or DC treated with TNF-α (TNFα-DC). In contrast to TNFα-DC (76.3 ± 1.3%) or LacZ-DC (82.0 ± 2.6%), CD154-DC (2×10^5) significantly suppressed the growth of OSC-70 cells to 50.6 ± 1.2% (Figure 2a, $n = 3$, $P < 0.05$). Furthermore, the low DC to OSC-70 ratio of 1:8 was still effective in suppressing tumor growth *in vitro*.

To determine whether the growth inhibitory effect by CD154-DC was caused through DC-tumor cell interaction, OSC-70 cells were co-cultured with DC in a dual-chamber transwell plate separated by a 0.4-μm pore size semi-permeable membrane. As shown in Figure 2b, the cell growth of OSC-70 cells co-cultured with CD154-DC (2×10^5) in a transwell plate were suppressed to similar levels as the mixed co-cultivation (51.4 ± 1.5%, $n = 3$, $P < 0.05$). These results indicate that the tumor growth inhibitory effect induced by CD154-DC could be caused by soluble factors secreted from DC and that it was independent of DC-tumor cell contact.

CD154-DC upregulated the TRAIL susceptibility of tumor cells

To investigate whether CD154-DC can alter the susceptibility to apoptosis inducing stimuli on co-cultured tumor cells, we analyzed the TRAIL-mediated apoptosis of tumor cells following co-cultivation with CD154-DC. We first examined the viability of CD154-DC co-cultured OSC-70 cells after treatment with recombinant TRAIL. As shown in Figure 3a, the viability of OSC-70 cells co-cultured with CD154-DC compared to LacZ-DC was significantly decreased after treatment with recombinant TRAIL in a dose-dependent manner ($n = 3$, $P < 0.05$ for all concentrations of TRAIL used).

To assess another indicator of apoptosis, we next examined DNA fragmentation of CD154-DC co-cultured OSC-70 cells using the Br-dUTP uptake assay. The percentage of cells containing fragmented DNA after treatment with recombinant TRAIL following co-cultivation with CD154-DC was increased 10-fold as compared to controls (Figure 3b).

CD154-DC induced surface antigen molecules on tumor cells

Expression levels of TRAIL-R1 (*DR4*) and TRAIL-R2 (*DR5*) are important to induce TRAIL-mediated apoptosis.[13,14] Previous reports showed that increasing *DR5* gene expression can increase TRAIL-induced apoptosis.[15–17] Thus, we examined whether CD154-DC can increase levels of apoptosis by inducing death receptors such as TRAIL-R1, TRAIL-R2 and Fas. OSC-70 cells co-cultured with CD154-DC were evaluated for the expression of TRAIL-R1, TRAIL-R2 and Fas. In contrast to OSC-70 cells co-cultured with LacZ-DC, OSC-70 cells co-cultured with CD154-DC expressed high levels of TRAIL-R2 (Figure 4).

Human leukocyte antigen (HLA)-class I, HLA-class II and intercellular adhesion molecule 1 are necessary for recognition of tumor cells by immune effector cells.[18–22]

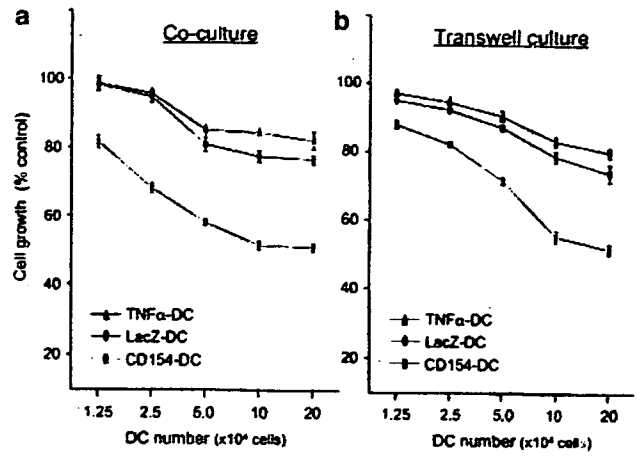

Figure 2 Assessment of growth of OSC-70 cells co-cultured with CD154-dendritic cells (DC). OSC-70 cells (1×10^5) were co-cultured with CD154-DC at several DC/tumor ratios in a 12-well culture plate (a) or a 12-well transwell culture plate (b) for 48 h. As controls, OSC-70 cells were also co-cultured with LacZ-DC or DC treated with tumor necrosis factor (TNF)-α (100 ng ml^{-1}) (TNFα-DC). A total of 48 h after co-cultivation, DC were discarded, and the viability of the adherent OSC-70 cells were measured by the WST-1 cell proliferation assay system. Mean values ± s.d. from triplicate determinations are shown. One of data in two independent experiments was represented.

Downregulation of these molecules was a frequent event observed in several tumors.[23,24] To investigate whether the phenotype of the tumor cells could be altered following co-cultivation with CD154-DC, we measured surface levels of immune co-stimulatory molecules. Following co-cultivation with CD154-DC in transwell plates, HLA-class I, HLA-class II and CD54 levels expressed on OSC-70 cells were evaluated by flow cytometry. In contrast to controls, OSC-70 cells co-cultured with CD154-DC expressed high levels of HLA-class I and CD54 (Figure 4). Importantly, HLA-class II expression on OSC-70 cells, which is normally very low, was highly induced by co-cultivation with CD154-DC.

CD154-DC, but not LPS- or TNFα-DC, induced growth suppression of tumor cells

It has been shown that molecules in the TNF family or ligands of Toll-like receptors contribute to the maturation and activation of DC. We next examined the induction of growth suppression of OSC-70 by DCs with various stimuli. Compared with immature DC, the addition of TNF-α or LPS could upregulate the expression of CD80 as a maturation/activation marker of DC (MFI CD80: 58 vs 134 and 402; Figure 5a). Adenovirus-mediated gene transfer of lacZ did not induce DC maturation, whereas CD154 could upregulate the CD80 expression (MFI CD80: 60 vs 293), indicating that DC stimulated with LPS (LPS-DC) could express significantly higher levels of CD80 than those stimulated with TNF-α or CD154. It is important that growth suppression of tumor cells were strongly induced only by CD154-DC but not by im-DC, TNFα-DC or LacZ-DC (Figure 5b). In contrast to the phenotypic changes in DC, LPS-DC could inhibit tumor growth moderately. Conceivably, signal transduction

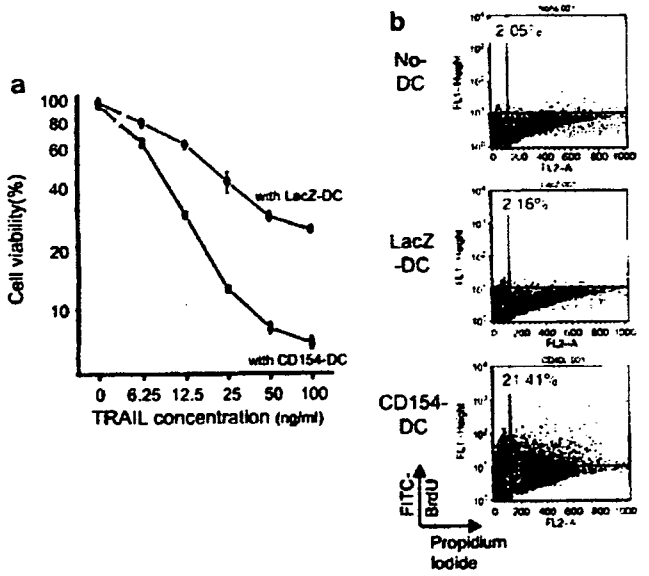

Figure 3 TNF-related apoptosis inducing ligand (TRAIL)-mediated cell death of OSC-70 cells co-cultured with CD154-dendritic cells (DC). (a) Cell viability of OSC-70 cells treated with recombinant TRAIL following co-cultivation with CD154-DC. OSC-70 cells were co-cultured with either LacZ-DC or CD154-DC in a dual-membrane transwell plate. A total of 48 h after co-cultivation, OSC-70 cells were collected and seeded into 96-well plates at 1.5×10^4 cells. After 24 h, OSC-70 cells were treated with increasing concentrations (6.25, 12.5, 25, 50 and 100 ng ml^{-1}) of recombinant TRAIL. A total of 48 h after TRAIL treatment, the viability of OSC-70 cells were measured by the WST-1 cell proliferation assay system. Mean values ± s.d. from triplicate determinations are shown. (b) The DNA fragmentation of OSC-70 cells treated with recombinant TRAIL following co-cultivation with CD154-DC. A total of 48 h after co-cultivation, OSC-70 cells were collected and replated onto a 60 mm dish. After 24 h, OSC-70 cells were treated with recombinant TRAIL (12.5 ng ml^{-1}). A total of 24 h after TRAIL treatment, DNA fragments in apoptotic cells were detected using the APO-BRDU kit. The *x* axis represents the propidium iodide-related fluorescence and the *y* axis represents the Br-dUTP-related fluorescence. FITC-BrdU positive cells in upper left and right regions indicate apoptotic cells with fragmented DNA. The percentage of apoptotic cells with fragmented DNA is shown in each panel.

mediated by CD154 or LPS in DC might be distinct between phenotypic alterations in immune response and cytostatic activity against tumors.

IFN-γ produced by CD154-DC mediated the growth suppression and TRAIL susceptibility of tumor cells

Recently, the susceptibility to TRAIL was shown to be induced by IFN-γ.[25,26] Stimulation with CD154 has also been shown to increase TNF-α- or FasL-mediated apoptosis of CD40-expressing tumor cells.[27,28] Since OSC-70 cells express CD40 (Tomihara *et al.*, unpublished observation), this may be a possible mechanism for the enhancement of TRAIL-mediated apoptosis. Thus, from cultures, we measured IFN-γ, IL-12p70 and soluble CD154 levels by ELISA. As shown in Figure 6, the IFN-γ concentration was 11-fold higher in CD154-DC supernatants (18.38 ± 0.73 ng per 10^6 cells per 48 h) than in LacZ-DC supernatants (1.67 ± 0.03 ng per 10^6 cells per 48 h). CD154 levels were 13-fold higher in CD154-DC supernatants (9.65 ± 0.41 ng per 10^6 cells per 48 h) as compared to the control (0.71 ± 0.54 ng per 10^6 cells per 48 h). Similarly, CD154-DC could produce large amount of IL-12p70 in the culture supernatant (2.22 ± 0.34 ng per 10^6 cells per 48 h). These data led us to believe that CD154-DC-secreted IFN-γ, IL-12p70 or soluble CD154 might be responsible for augmentation of TRAIL-induced apoptosis in the tumor cells co-cultured with CD154-DC.

To evaluate the contribution of these cytokines in tumor growth arrest and TRAIL susceptibility, we examined the growth of OSC-70 cells co-cultured with CD154-DC in the presence or absence of a neutralizing antibody to IFN-γ (anti-IFN-γ Ab) or CD154 (anti-CD154 Ab). Anti-IFN-γ Ab, but not anti-CD154 Ab blocked CD154-DC-induced growth suppression of OSC-70 cells (data not shown). We next examined the TRAIL susceptibility of OSC-70 cells co-cultured with CD154-DC in the presence or absence of an anti-IFN-γ Ab or an anti-CD154 Ab. Anti-IFN-γ Ab blocked the TRAIL-induced cell death of CD154-DC co-cultured OSC-70 cells partially, but significantly at all TRAIL concentrations tested (Figure 7a) ($n = 3$, $P < 0.05$ for all concentrations of TRAIL). In contrast, anti-CD154 Ab had no effect on TRAIL-induced cell death of CD154-DC co-cultured OSC-70 cells (Figure 7b).

We then examined whether cytostatic activity of CD154-DC could be replaced by the addition of recombinant human IFN-γ (rhIFN-γ). As represented in Figure 7c, growth inhibition of OSC-70 cells with 25% of CD154-DC supernatant containing IFN-γ at 2750 pg ml^{-1} was definitely observed (34.7% vs control culture). In contrast, the addition of equal amounts of rhIFN-γ (2750 pg ml^{-1}) to medium or LacZ-DC supernatants partially inhibited tumor cell growth (65.1 or 75.3% vs control culture), indicating that additional rhIFN-γ did not fully take the place of CD154-DC. In addition to above results, the upregulation of TRAIL susceptibility by co-cultivation with CD154-DC were also observed in CD40-negative tumor cells (data not shown). In preliminary data, we found that immunostimulatory cytokine IL-12p70 could not induce the tumor growth arrest and phenotypic alterations. Collectively, these results suggest that CD154-DC-derived IFN-γ but not soluble CD154 nor IL-12p70, at least in part, mediates CD154-DC-mediated tumor growth suppression and susceptibility of apoptosis via TRAIL.

JAK-STAT signaling is an important pathway in the induction of several pro-apoptotic effects by IFNs.[29,30] Moreover, sensitivity to TRAIL-induced apoptosis in tumor cells was regulated by altering the levels of TRAIL receptors,[15–17] and of anti-apoptotic molecules such as Fas-associated death domain-like interleukin-1β-converting enzyme (FLICE) inhibitor protein (FLIP)[31] or death-associated protein-3 (DAP3).[32] Post-translational modification of anti-apoptotic molecules such as Akt also contribute to TRAIL-induced apoptosis.[33–36] To investigate whether expression levels of molecules relating to TRAIL-mediated apoptosis were affected when OSC-70 cells were co-cultured with CD154-DC, we performed western blot analyses of STAT-1, Akt, Ser473-phosphorylated Akt, cFLIP and DAP3. As shown in Figure 7D, upregulation of STAT-1 and downregulation of Akt phosphorylation were observed in OSC-70 cells following co-cultivation with CD154-DC. The neutralizing anti-IFN-γ Ab attenuated these changes. No remarkable

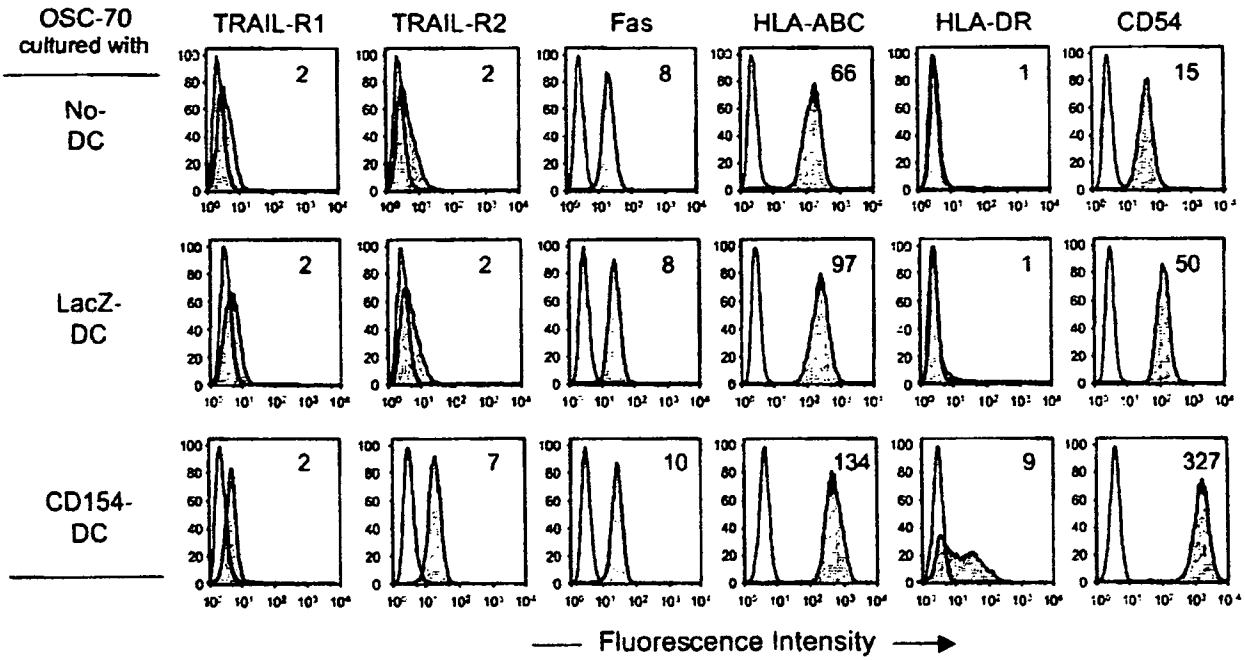

Figure 4 Expression of TNF-related apoptosis inducing ligand (TRAIL)-receptors and co-stimulatory molecules on OSC-70 cells co-cultured with CD154-dendritic cells (DC). OSC-70 cells were co-cultured with either LacZ-DC or CD154-DC in a 12-well transwell culture plate. A total of 48 h after co-cultivation, OSC-70 cells were stained with antibodies against TRAIL-DR4, TRAIL-DR5, Fas, HLA-ABC, HLA-DR and CD54, respectively. Their expression levels were quantified via flow cytometry. Open histograms represent staining of OSC-70 cells with anti-human IgG negative control mAb. Oblique-lined histograms represent staining of OSC-70 cells with FITC- or PE-conjugated mAb. The number in each panel represents the mean fluorescence intensity ratio. One of data in three independent experiments was represented.

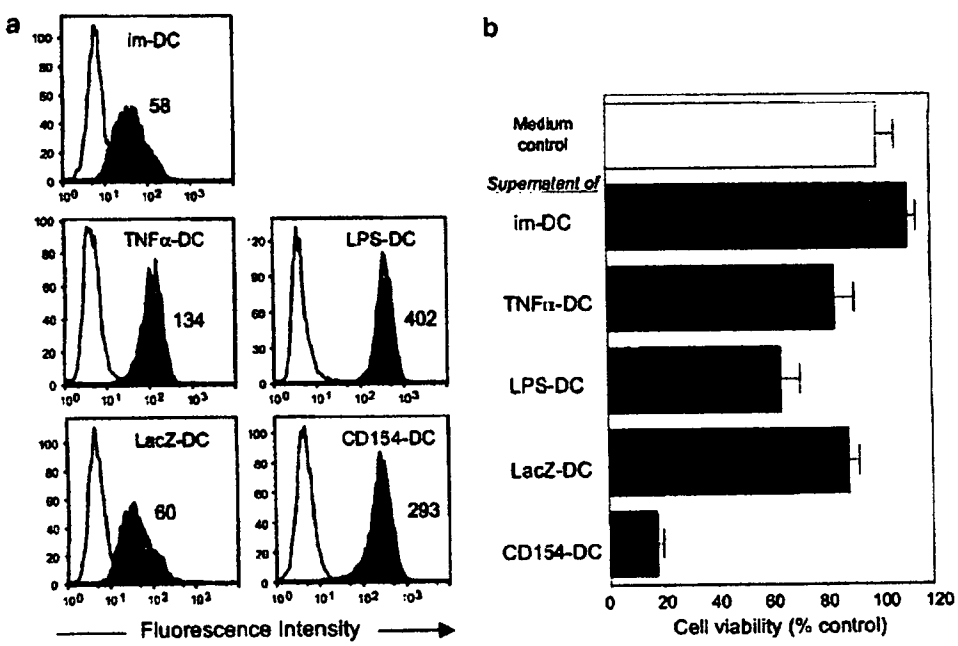

Figure 5 Dendritic cells (DC) activation and tumor growth suppression by various stimulation. (a) Phenotypic alteration of DC stimulated with tumor necrosis factor (TNF)-α (100 ng ml^{-1}), lipopolysaccharide (LPS) (1 μg ml^{-1}) or transfected with adenovirus vector encoding LacZ or CD154 at 1000 pt per cell for 48 h. Surface expression of CD80 on DC was measured by flow cytometry. Mean fluorescence Intensity values of each DC are indicated. (b) Growth suppression of OSC-70 cells cultured with various DCs. OSC-70 cells (2×10^5) were co-cultured with immature-DC (im-DC), TNFα-DC, LPS-DC, LacZ-DC or CD154-DC at a DC/tumor ratio of 1:1 in a 12-well transwell culture plate. A total of 48 h after co-cultivation, the viability of OSC-70 cells were determined by the WST-1 cell proliferation assay system. One of data in two independent experiments was represented.

changes in protein expression of cFLIP or DAP3 were observed. These results suggest that upregulation of STAT-1 and downregulation of Akt phosphorylation upon IFN-γ secretion by CD154-DC may mediate TRAIL-induced apoptosis of tumor cells co-cultured with CD154-DC.

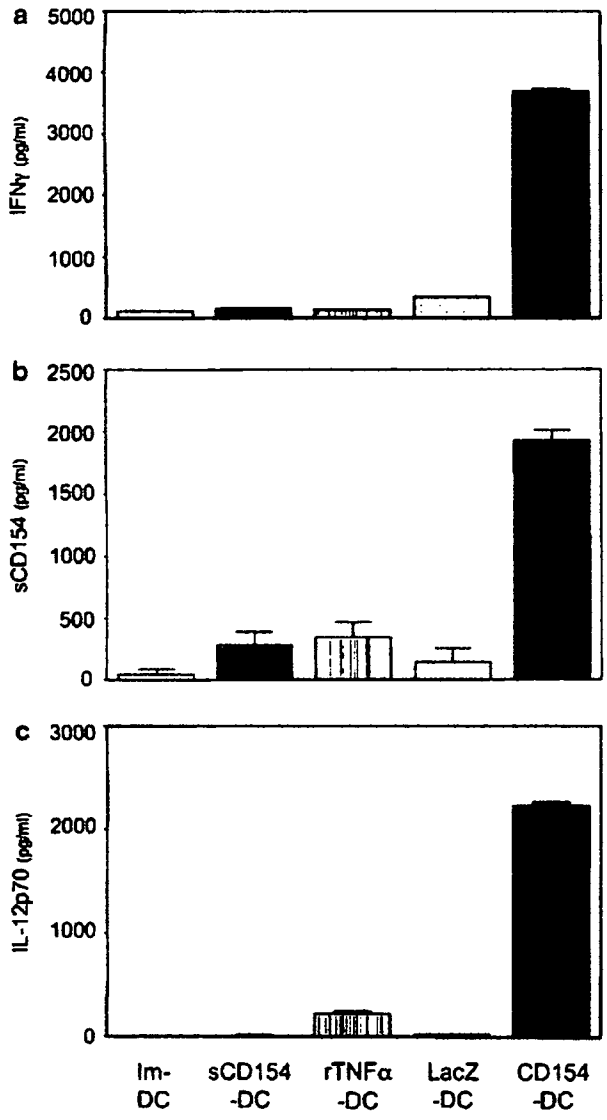

Figure 6 Cytokine production by CD154-dendritic cells (DC). Immature dendritic cells derived from PBMC from a healthy donor were infected with Adv-CD154 or Adv-LacZ. After 48 h post-infection interferon (IFN)-γ (a), soluble CD154 (b) and IL-12p70 (c) concentrations in supernatants of 2×10^5 dendritic cells per ml were determined by ELISA. In addition to Adv-infected-DC, supernatants of DC treated with recombinant tumor necrosis factor (TNF)-α (100 ng ml^{-1}) or CD154 (100 ng ml^{-1}) were also measured. One of data in two independent experiments was represented.

In vivo *efficacy of CD154-DC to treat established oral squamous cell carcinoma xenograft*

Based on the biological activity of CD154-DC *in vitro*, we evaluated the antitumor efficacy of CD154-DC treatment in OSC-70 xenografts. Athymic nude mice bearing subcutaneously (s.c.) OSC-70 were injected intratumor for once a week three times with CD154-DC, LacZ-DC or phosphate-buffered saline (PBS) and tumor growth was monitored for up to 30 days after the initial treatment. There was no significant effect on growth kinetics in tumors treated with LacZ-DC compared with control mice. In contrast to no therapeutic effect of LacZ-DC, a potent antitumor effect of CD154-DC became apparent 5 days after treatment, and this effect was sustained over the treatment (Figure 8). However, all mice treated with CD154-DC exhibited tumor regrowth after second or third treatment. Student's *t*-test analysis of the data of tumor volume (day 30) and tumor weight (day 35) revealed that the difference between the CD154-DC-injected and LacZ-DC-injected groups were significant ($P<0.05$). Collectively, these results indicated that CD154-DC exhibit potent antitumor property against tumor xenograft.

Discussion

Several reports have shown that adenovirus-mediated murine CD154 gene transduction to DC induce anti-tumor effect following generation of tumor-specific CTL.[37,38]

In the present study, we developed the modified adenovirus vectors encoding human CD154 gene to enable the superior gene transduction efficiency against DC and demonstrated that adenovirus-mediated transduction of the human CD154 gene to DC imparts a direct antitumor effect. By co-culturing in a transwell plate, we demonstrated that DC transduced with the CD154 gene (CD154-DC) suppressed growth of tumor cells without cell-to-cell contact. In addition to inhibiting tumor cell growth, TRAIL-mediated apoptosis was strongly induced in tumor cells following co-cultivation with CD154-DC. These results suggest that these cytostatic and cytotoxic effects toward tumor cells could be caused by soluble factors secreted by CD154-DC. DC are major producers of IFNs. Virally infected $CD11c^-$ precursor DC release type 1 IFNs.[7,8] It has also been reported that murine lymphoid DC stimulated with IL-12 or IL-18 can release IFN-γ.[11] However, there is no report that human DC can produce this cytokine. In the present study, we have shown that CD154 transduction of human DC by adenovirus vectors can cause secretion of IFN-γ. In addition, stimulation with recombinant CD154, TNF-α or LPS did not increase production of IFN-γ and not inhibit tumor cell growth. These results suggest that it is important to stably express CD154 on cell membranes by gene transduction to stimulate DC IFN-γ production.

Recently, it was recognized that IFNs are major modulators of death inducing stimuli such as FasL or TRAIL. It was reported that a combination of TRAIL receptor agonists and IFN-γ treatment could induce apoptosis of TRAIL resistant tumor cells.[26] As shown in our data (Figure 6), CD154-DC secreted higher amounts of IFN-γ compared with LacZ-DC. We also demonstrated that TRAIL-mediated cell death of OSC-70 cells following co-cultivation with CD154-DC was attenuated by blocking IFN-γ with a specific antibody. IFNs are also known to exert several pro-apoptotic effects through the JAK-STAT signaling pathway.[29] More recently, it was found that type 1 IFNs stimulation induced a STAT-1-dependent TRAIL-mediated death signaling pathway.[30] In accordance with this data, we demonstrated that expression of STAT-1 protein was increased in OSC-70 cells following co-cultivation with CD154-DC. Further, this increase could be attenuated by blocking IFN-γ with a specific antibody. These data suggest that TRAIL-induced apoptosis of OSC-70 cells following co-cultivation with CD154-DC could be upregulated by

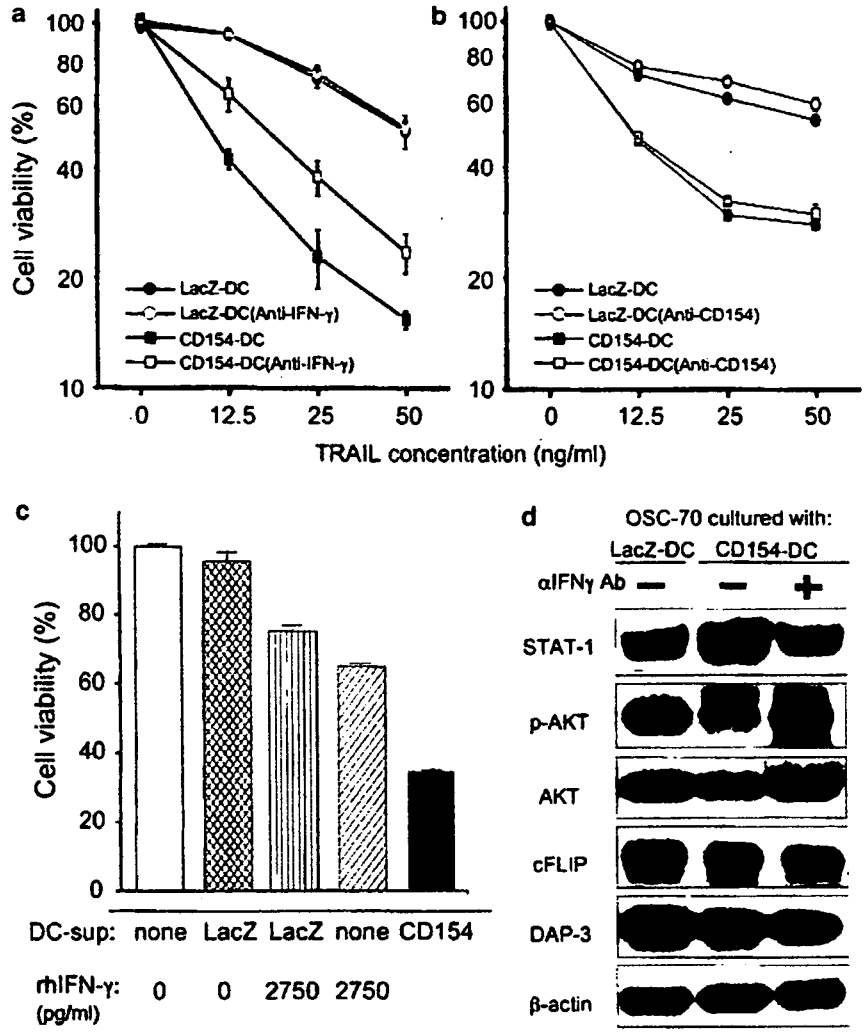

Figure 7 Contribution of interferon (IFN)-γ produced by CD154-dendritic cells (DC) in tumor growth suppression and TNF-related apoptosis inducing ligand (TRAIL) susceptibility. (a, b) OSC-70 cells were co-cultured with either LacZ-DC or CD154-DC in a 12-well transwell culture plate in the presence or absence of a neutralizing antibody to IFN-γ (a) or to CD154 (b) at 10 μg ml^{-1}. A total of 48 h after co-cultivation, OSC-70 cells were replated into 96-well plates. A total of 24 h after replating, OSC-70 cells were treated with recombinant TRAIL (12.5, 25 and 50 ng ml^{-1}) for 48 h and then the viability were determined by the WST-1 cell proliferation assay system. One of data in two independent experiments was represented. (c) OSC-70 cells (1 × 10^4) were co-cultured without or with 20% of supernatants derived from LacZ-DC or CD154-DC in a 96-well transwell culture plate. In addition to LacZ-DC supernatant or medium, recombinant human IFN-γ (2750 pg ml^{-1}) was added into cultures. A total of 48 h after co-cultivation, the viability of OSC-70 cells were determined by the WST-1 cell proliferation assay system. (d) *Immunoblot analysis of STAT-1, Akt phosphorylation, cFLIP and DAP3 proteins in OSC-70 cells co-cultured with CD154-DC.* Proteins were extracted from OSC-70 cells 48 h after co-cultivation with either LacZ-DC or CD154-DC. When co-cultivated with CD154-DC, OSC-70 cells were cultured in the presence or absence of a neutralizing antibody to IFN-γ.

CD154-DC-derived IFN-γ. However, the addition of equal amounts of recombinant IFN-γ to LacZ-DC supernatants was not fully replaced in the tumor cell growth arrest induced by CD154-DC (Figure 7c). These data indicate that CD154-DC may produce other candidate factors for modulating tumor cell growth. We measured the levels of two other potential contributors. First, type 1 IFNs (α2b and β) were undetectable in supernatants of both LacZ-DC and CD154-DC cultures. The second potential contributor, CD154, however, was increased in the culture supernatant of CD154-DC (Figure 6). In support of this notion, stimulation of CD40 positive tumor cells with CD154 suppressed tumor growth, increased chemotherapy sensitivity and enhanced apoptosis by apoptosis inducing stimuli such as TNF-α or FasL.[27,28] While the CD154 detected in the culture supernatant may be a soluble form (sCD154) cleaved from CD154-DC, it is not clear whether it has the same functional activity as recombinant CD154 or as cells expressing CD154 on their surfaces. However, OSC-70 cells express CD40, this may be a possible mechanism for the enhancement of TRAIL-mediated apoptosis. However, as shown in our data, upregulation of TRAIL susceptibility of OSC-70 cells following co-cultivation with CD154-DC could not be attenuated by using a neutralizing antibody to CD154 (Figure 7b). In addition, CD154-DC also induced TRAIL susceptibility on CD40-negative tumor cells (data not shown). Thus, it is unlikely that sCD154 contributes to the TRAIL susceptibility of tumor cells. Immunostimulatory cytokine IL-12p70 was abundantly produced by CD154-DC compared with TNFα-DC or LPS-DC; however, we

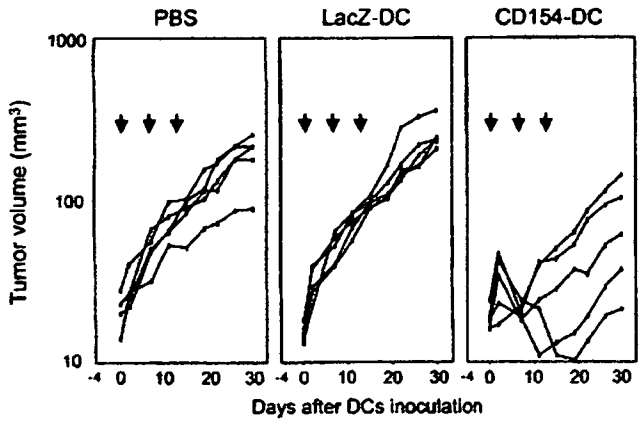

	PBS	LacZ-DC	CD154-DC
Tumor volume (mm³) at day 30	190.4 ± 63.2	255.1 ± 58.5	73.1 ± 49.2*
Tumor weights (mg) at day 35	178.9 ± 37.7	224.3 ± 83.6	84.5 ± 55.2*

Figure 8 Tumor growth suppression by CD154-dendritic cells (DC) in established OSC-70 xenograft model. OSC-70 tumors (1×10^6) were inoculated s.c. into athymic mice. After 4 days, tumor-bearing mice were randomized into three groups as indicated. Intratumoral injection of phosphate-buffered saline (PBS), LacZ-DC or CD154-DC (5×10^5 per mouse) was performed once a week as shown as an arrow. Diameters of tumor nodules were measured and calculated as tumor volume. Data of tumor volume (day 30) and weights (day 35) represent the mean ± s.d. of five mice in each group. Asterisk (*) indicates significantly difference ($P<0.05$, Student's *t*-test) between CD154-DC- and LacZ-DC-treated groups.

observed that IL-12p70 could not induce phenotypic changes nor growth arrest of OSC-70. Further studies are required to determine whether the unknown factors secreted by CD154-DC contribute to the direct growth arrest and TRAIL susceptibility of tumor cells.

Several molecules have been reported to correlate with TRAIL susceptibility. FLIP is recognized to be one of these proteins. It was reported that high expression of FLIP correlated to TRAIL-resistant melanomas.[31] More recently, it was reported that DAP3, a GTP-binding protein that binds directly to the death domain of TRAIL receptors, is required for TRAIL-induced apoptosis. DAP3 also associates with the pro-caspase-8 binding adapter protein Fas-associated death domain (FADD) and links FADD to the TRAIL receptors DR4 and DR5.[32] Resistance to TRAIL-mediated apoptosis has been attributed to differential expression of TRAIL receptors (DRs).[15–17] OSC-70 cells following co-cultivation with CD154-DC upregulated TRAIL-R2 expression. However, western blot analysis for cFLIP and DAP3 revealed no remarkable changes in expression levels following co-cultivation with CD154-DC. Thus, the secretion of soluble factors by CD154-DC did not affect the expression of these proteins in OSC-70 cells. Further study is needed in order to shed light on the mechanism involved. Other possibilities include a change in the phosphorylation state or intracellular localization of these molecules and/or the involvement of anti-apoptotic molecules other than those already studied. In addition to alterations of these molecules, constitutive phosphorylation of Akt may contribute to the resistance of TRAIL-induced cell death. Akt is a Ser/Thr protein kinase activated in many cancers. It has been reported that activation of Akt promotes tumor cell growth, inhibition of apoptosis and drug resistance.[39,40] Several cancer cells with high levels of Akt activity were resistant to TRAIL-induced apoptosis.[33–36] As shown in our data (Figure 7d), OSC-70 cells co-cultured with CD154-DC downregulated Akt phosphorylation. Therefore, disruption of Akt signaling may be an effective way to treat many cancers.

In this study, we have demonstrated that human DC infected with Adv-CD154 (CD154-DC) suppressed tumor cell growth and enhanced TRAIL susceptibility. As expected, CD154-DC exhibited potent antitumor property in OSC-70-bearing mice. We also observed a therapeutic effect of CD154-DC against human renal carcinoma ACHN xenograft (data not shown). Considered together, CD154-DC could be a useful tool for cancer therapy; however, it would probably be most effective in combination with recombinant TRAIL or an agonistic monoclonal antibody specific for TRAIL receptors. A candidate source for TRAIL is the naturally occurring amount found on the cell surface of immune effector cells such as CTL and NK. Our results indicate that CD154-DC produce a large amount of IL-12, which is also a potent soluble factor to activate T helper-1, CTL and NK cells. In addition, high levels of IFN-γ were reproducibly secreted by CD154-DC. Smyth *et al.*[41] previously demonstrated that TRAIL induction on NK cells plays a critical role in IFN-γ-mediated anti-metastatic effects of IL-12. We also found that culturing the NK cells with CD154-DC significantly induced the expression of TRAIL on the cell surface (unpublished results). We are now investigating the antitumor effect of NK cells expressing TRAIL in combination with CD154L-DC *in vitro* and *in vivo*. In conclusion, DC transfected with stable CD154 may be more efficient at inducing both direct cytostatic and apoptosis-inducing effects toward tumor cells as well as indirect immune responses mediated by NK and CTLs. The next step of our research is to verify the antitumor efficacy in immunocompetent animal model. Thus, this approach may be a viable immune gene therapy for cancer patients.

Materials and methods

Preparation of DC

Human peripheral blood mononuclear cells were donated from healthy donors. In brief, non-adherent cells were depleted, and adherent cells were cultured in complete RPMI-1640 medium (containing 1 mM sodium pyruvate, antibiotics and 10% fetal calf serum (FCS)) supplemented with recombinant human granulocyte macrophage-colony stimulating factor and IL-4 (Osteogenetics GmbH, Wuerzburg, Germany) at a concentration of 50 ng ml^{-1} for 7 days.

Tumor cells

The human oral squamous cell carcinoma cell line, OSC-70, established from a metastatic oral squamous carcinoma as described previously[42] was maintained in complete RPMI-1640 medium.

Culture experiments

To co-cultivate OSC-70 cells with DC, we used a dual-chamber transwell plate separated by a 0.4-μm pore size

semi-permeable membrane (12-well plate, Corning Inc., Corning, NY, USA).

Adenovirus

All the recombinant adenoviral vectors used in this study were based on the E1- and E3-deleted serotype 5 adenovirus with a modified fiber F/RGD, harboring an integrin-binding RGD-motif within the HI loop of its knob protein.[43] In the first step, a 14 896-bp *Eco*RI fragment (including the right side of the adenoviral genome) of pWEAxKM-F/RGD[43] was joined with a 24 505-bp *Eco*RI fragment (including the left side of the adenoviral genome) of pL_{RI},[44] generating the cosmid vector pWEAx-F/RGD.

Human CD154 cDNA was cloned by RT–PCR using total RNA extracted from activated human T cells of healthy donors. The human CD154 primer sequences were: Forward, 5′-CGG AAT TCA GCA TGA TCG AAA CAT ACA ACC AAA C-3′ Reverse, 5′-CGG GAT CCT CAG AGT TTG AGT AAG CCA AAG GAC G-3′.

The human CD154 cDNA was inserted between the *Eco*RI and *Bgl*II sites in the pCAcc vector, and the resulting plasmid was designated pCAhCD154. Then, pCAhCD154 was digested with *Cla*I, and the CD154 expression unit was inserted into the *Cla*I site of pWEAx-F/RGD, resulting in the cosmid vectors pWEAx-CAhCD154-F/RGD. To generate recombinant adenovirus, *Pac* I-digested cosmid was transfected into 293 cells with Lipofectamine2000 reagent (Invitrogen, Carlsbad, CA, USA). Resulting plaques were isolated, and they were evaluated by restriction enzyme digestion of the viral genome. Similarly, AxCAZ3-F/RGD that carried *lacZ* as a reporter gene was generated. The resulting adenoviral vectors, AxCAhCD154-F/RGD (Adv-CD154) and AxCAZ3-F/RGD (Adv-LacZ) were amplified in 293 cells and purified by cesium chloride ultracentrifugation.[45] Purified viruses were dialyzed against PBS with 10% glycerol and stored at −70 °C until use. To determine the viral concentration (particle per ml), the viral solution was incubated in 0.1% sodium dodecyl sulfate (SDS) and its absorbance was measured at A_{260}.[46] The concentration was defined as pt per ml = $A_{260} \times (1.1 \times 10^{12})$. Before use, contamination of the viral stocks with replication-competent viruses was ruled out by PCR analysis using primers specific for E1A and E1B.[47]

Adenovirus infection

DC were infected with adenovirus using 1000 pt per cell to achieve nearly 100% infection efficiency. After 48 h of adenovirus infection, DC were evaluated for maturation markers by flow cytometry. In all of the assays, DC were used 48 h post-infection.

Reagents and neutralizing antibodies

Recombinant TNF-α (rhTNF-α), IFN-γ (rhIFN-γ) and CD154 (rhCD154) proteins were purchased from PeproTech (London, UK), R&D systems (Minneapolis, MN, USA) and Alexis Corporation (San Diego, CA, USA), respectively. Monoclonal antibodies specific for human IFN-γ (anti-IFN-γ Ab) or CD154 (anti-CD154 Ab) were purchased from BD-PharMingen (San Diego, CA, USA).

Flow cytometry

Cells were washed and then suspended in staining media (PBS, 2% FCS, 0.05%. NaN_3 and 1 mg ml^{-1} propidium iodide (PI)) containing saturating amounts of fluorochrome-conjugated mAbs. After 30 min at 4 °C, the cells were washed with staining media and analyzed by flow cytometry using a FACS-Calibur (Becton Dickinson, San Jose, CA, USA). Dead cells staining with PI were excluded from the analysis. The relative expression of surface antigen is described as the mean fluorescence intensity ratio (mean fluorescence intensity ratio (MFIR)). MFIR equals the MFI of cells stained with a fluorochrome-conjugated antigen-specific mAb divided by the MFI of cells stained with a fluorochrome-conjugated isotype control mAb. Fluorescein (FITC)-conjugated mAbs specific for human CD54 were purchased from Caltag (Burlingame, CA, USA). Fluorescein (FITC)-conjugated mAb specific for human CD80, CD86, CD95, CD154 or HLA-DR, DP, DQ and phycoerythrin (PE)-conjugated mAb specific for HLA-ABC were obtained from BD-PharMingen. Fluorescein (FITC)-conjugated mAb specific for human TRAIL-R1 (DR4) or TRAIL-R2 (DR5) were obtained from Alexis. PE-conjugated mAb specific for human CD83 was purchased from Immunities (Marselle, France).

Cytokine ELISA

Supernatants of DC were collected 48 h after infection with Adv-LacZ or Adv-CD154. Cytokine levels were measured using ELISA kits specific for IFN-γ (eBioscience, San Diego, CA, USA), IL-12p70 (R&D systems), CD154, IFN-α or IFN-β (PBL Biomedical Laboratories, Piscataway, NJ, USA) according to manufacturer's instructions at 450 nm.

Immunoblot analysis

Cells were lysed with 1 × lysis buffer (10 mm Tris-HCl (pH 7.4), 1% SDS, 1 mm sodium orthovanadate). The protein content of the supernatants was determined using the DC protein assay kit (Bio-Rad, Hercules, CA, USA) according to the manufacturer's instructions. An equal volume of 2 × Laemmli buffer was added to the supernatants and boiled for 5 min. Equal amounts of protein (30 μg) were separated using 5–20% gradient polyacrylamide gels and transferred onto nitrocellulose membranes. After blocking with 5% milk in Tris-buffered saline 10 mm Tris-HCl (pH 7.5), 150 mm sodium chloride, 0.05% Tween-20) the membranes were incubated with primary antibodies for 1 h at room temperature. Primary antibodies used included mouse anti-human STAT-1 monoclonal antibody (no. 9176; Cell Signaling Technology, Beverly, MA, USA), rabbit anti-human Akt polyclonal antibody (no 9272; Cell Signaling Technology), mouse anti-human phospho-Akt (Ser473), or mouse anti-β-actin monoclonal antibody (no. A-5441; Sigma, St Louis, CA, USA), rabbit anti-human-FLIPγ/δ polyclonal antibody (no. 343006, Calbiochem, Darmstadt, Germany) or mouse anti-human DAP3 monoclonal antibody (no. 9176; BD PharMingen, San Diego, CA, USA). After washing, the membranes were incubated for 1 h at room temperature with 30 μl (per 15 ml) of horseradish peroxidase-conjugated rabbit anti-mouse IgG+A+M (H+L) (no. 61-6420; Zymed Laboratories, San Francisco, CA, USA) or donkey anti-rabbit IgG,

peroxidase-linked species-specific F(ab')2 fragment (Amersham. Little Chalfont, UK). Detection was carried out by enhanced chemi-luminescence (Amersham) according to the manufacturer's instructions.

Assessment of cell viability

Cells were seeded into 96-well plates at 1.5×10^4 cells per well 1 day prior to the experiment. Cells were treated with increasing concentrations (6.25, 12.5, 25, 50 and 100 ng ml^{-1}) of recombinant TRAIL (R&D). To measure the viability of adherent cells, tetrazolium salt WST-1 (4-[3-(4-iodophenyl)-2-(4-nitrophenyl)-2H-5-tetrazolio]-1, 3-benzene disulfonate) premix (Takara Bio, Otsu, Shiga. Japan) was added to each well. The cleavage of WST-1 into formazan by metabolically active cells was measured by scanning the plates at 450 and 650 nm reference wavelengths in a microtiter plate reader.

Assessment of apoptosis

OSC-70 cells co-cultured in transwell dishes with DC were replated onto 60 mm dishes. After 24 h, OSC-70 cells were treated with recombinant human TRAIL at a concentration of 12.5 ng ml^{-1}. After another 24 h, DNA fragments in apoptotic cells were detected using the APO-BRDU kit (BD PharMingen) according to the manufacturer's instructions. The kit is a two color TUNEL assay for labeling DNA breaks by Br-dUTP plus FITC-anti-BrdU antibody and total cellular DNA by PI.

Xenograft studies

Female athymic KSN-slc nude mice, 6–8 weeks of age, were purchased from Japan SLC Inc. (Shizuoka, Japan) and housed at the Sapporo Medical University animal facility. This animal studies were approved by the Animal Subject Committee (protocol no. 07–022) and the Biosafety Committee (approval no. Sapmed-1043) of the Sapporo Medical University and were performed in accordance with institutional guidelines.

OSC-70 cells in cultures were trypsinized, washed and resuspended with PBS. The viable OSC-70 cells (1×10^6) were transplanted s.c. into the left flank of the athymic mice. After 4 days, mice were randomized into the three groups: (1) PBS as control, (2) LacZ-DC and (3) CD154-DC ($n = 5$ in each group), and treatment was initiated (day 0). LacZ-DC or CD154 (5×10^5) was injected i.t. once a week for 3 weeks and mice were monitored twice weekly until day 35. Tumor diameters were serially measured with digital calipers, and the tumor volume was estimated using the following formula: tumor volume (mm^3) = (long diameter) × (short diameter)^2 × 0.4. A total of 39 days after tumor inoculation, all mice were euthanized and tumor tissues surgically obtained were weighed.

Statistical analysis

The statistical significance of the data was analyzed using a Student's *t*-test. A *P*-value of less than 0.05 was considered to be significant.

Acknowledgements

We thank Hokkaido Red Cross Blood Center for providing us with human peripheral blood, and Tomoko Sonoda for her analysis assistance.This work was supported by Grant-in-Aid for Scientific Research on Priority Areas 'Cancer' from the Ministry of Education, Culture, Sports, Science and Technology (K Kato, K Nakamura and H Hamada) and by Grant-in-Aid for Cancer Research from the Ministry of Health and Welfare of Japan (H Hamada) and by Grant-in-Aid from Japan Leukemia Research Fund (K Kato).

References

1 Albert ML, Sauter B, Bhardwaj N. Dendritic cells acquire antigen from apoptotic cells and induce class I-restricted CTLs. *Nature* 1998; 392: 86–89.
2 Griffith TS, Wiley SR, Kubin MZ, Sedger LM, Maliszewski CR, Fanger NA. Monocyte-mediated tumoricidal activity via the tumor necrosis factor-related cytokine, TRAIL. *J Exp Med* 1998; 189: 1343–1354.
3 Fanger NA, Maliszewski CR, Schooley K, Griffith TS. Human dendritic cells mediate cellular apoptosis via tumor necrosis factor-related apoptosis-inducing ligand (TRAIL). *J Exp Med* 1999; 190: 1155–1164.
4 Vidalain PO, Azocar O, Yagita H, Rabourdin-combe C, Servet-Delpart C. Cytotoxic activity of human dendritic cells is differentially regulated by double-stranded RNA and CD40 ligand. *J Immunol* 2001; 167: 3765–3772.
5 Chapoval AI, Tamada K, Chen L. In vitro growth inhibition of a broad spectrum of tumor cell lines by activated human dendritic cells. *Blood* 2000; 95: 2346–2351.
6 Caux C, Massacrier C, Vanbervliet B, Dubois B, Van Kooten C, Durand I *et al*. Activation of human dendritic cells through CD40 cross-linking. *J Exp Med* 1994; 180: 1263–1272.
7 Siegal FP, Kadowaki N, Shodell M, Fitzgerald-Bocarsly PA, Shah K, Ho S *et al*. The nature of the principal type 1 interferon-producing cells in human blood. *Science* 1999; 284: 1835–1837.
8 Palucka K, Banchereau J. Linking innate and adaptive immunity. *Nat Med* 1999; 5: 868–870.
9 Puddu P, Fantuzzi L, Borghi P, Varano B, Rainaldi G, Guillemard E *et al*. IL-12 induces IFN-gamma expression and secretion in mouse peritoneal macrophages. *J Immunol* 1997; 159: 3490–3497.
10 Munder M, Mallo M, Eichmann K, Modolell M. Murine macrophages secrete interferon gamma upon combined stimulation with interleukin (IL)-12 and IL-18: a novel pathway of autocrine macrophage activation. *J Exp Med* 1998; 187: 2103–2108.
11 Ohteki T, Fukao T, Suzue K, Maki C, Ito M, Nakamura M *et al*. Interleukin 12-dependent interferon gamma production by CD8alpha+ lymphoid dendritic cells. *J Exp Med* 1999; 189: 1981–1986.
12 Fukao T, Matsuda S, Koyasu S. Synergistic effects of IL-4 and IL-18 on IL-12-dependent IFN-gamma production by dendritic cells. *J Immunol* 2000; 164: 64–71.
13 Pan G, O'rourke K, Chinnaiyan AM, Gentz R, Ebner R, Ni J *et al*. The receptor for the cytotoxic ligand TRAIL. *Science* 1997; 276: 111–113.
14 Walczak H, Degli-Esposti MA, Johnson RS, Smolak PJ, Waugh JY, Boiani N *et al*. TRAIL-R2: a novel apoptosis-mediating receptor for TRAIL. *EMBO J* 1997; 16: 5386–5397.
15 Sheikh MS, Burns TF, Huang Y, Wu GS, Amundson S, Brooks KS *et al*. p53-dependent and -independent regulation of the death receptor KILLER/DR5 gene expression in response to genotoxic stress and tumor necrosis factor alpha. *Cancer Res* 1998; 58: 1593–1598.
16 Chinnaiyan AM, Prasad U, Shakar S, Hamstra DA, Shanaiah M, Chenevert TL *et al*. Combined effect of tumor necrosis factor-related apoptosis-inducing ligand and ionizing radiation in

breast cancer therapy. *Proc Natl Acad Sci USA* 2000; 97: 1754–1759.

17 Nagane M, Pan G, Weddle JJ, Dixit VM, Cavenee WK, Huang HJ *et al*. Increased death receptor 5 expression by chemotherapeutic agents in human gliomas causes synergistic cytotoxicity with tumor necrosis factor-related apoptosis-inducing ligand in vitro and in vivo. *Cancer Res* 2000; 60: 847–853.

18 Ferrone S, Marincola FM. Loss of HLA class I antigens by melanoma cells: molecular mechanisms, functional significance and clinical relevance. *Immunol Today* 1995; 16: 487–494.

19 Rivoltini L, Barracchini KC, Viggiano V, Kawakami Y, Smith A, Mixon A *et al*. Quantitative correlation between HLA class I allele expression and recognition of melanoma cells by antigen-specific cytotoxic T lymphocytes. *Cancer Res* 1995; 55: 3149–3157.

20 Topalian SL, Rivoltini L, Mancini M, Markus NR, Robbins PF, Kawakami Y *et al*. Human CD4+ T cells specifically recognize a shared melanoma-associated antigen encoded by the tyrosinase gene. *Proc Natl Acad Sci USA* 1994; 91: 9461–9465.

21 Marlin SD, Springer TA. Purified intercellular adhesion molecule-1 (ICAM-1) is a ligand for lymphocyte function-associated antigen 1 (LFA-1). *Cell* 1997; 51: 813–819.

22 Becker JC, Dummer R, Hartmann AA, Burg G, Schmidt RE. Shedding of ICAM-1 from human melanoma cell lines induced by IFN-gamma and tumor necrosis factor-alpha. Functional consequences on cell-mediated cytotoxicity. *J Immunol* 1991; 147: 4398–4401.

23 Garrido F, Ruiz-Cabello F, Cabrera T, Perez-Villar JJ, Lopez-Botet M, Duggan-Keen M *et al*. Implications for immunosurveillance of altered HLA class I phenotypes in human tumours. *Immunol Today* 1997; 18: 89–95.

24 Romero JM, Jimenez P, Cabrera T, Cozar JM, Pedrinaci S, Tallada M *et al*. Coordinated downregulation of the antigen presentation machinery and HLA class I/beta2-microglobulin complex is responsible for HLA-ABC loss in bladder cancer. *Int J Cancer* 2005; 113: 605–610.

25 Sedger LM, Shows DM, Blanton RA, Peschon JJ, Goodwin RG, Cosman D *et al*. IFN-gamma mediates a novel antiviral activity through dynamic modulation of TRAIL and TRAIL receptor expression. *J Immunol* 1999; 163: 920–926.

26 Merchant MS, Yang X, Melchionda F, Romero M, Klein R, Thiele CJ *et al*. Interferon gamma enhances the effectiveness of tumor necrosis factor-related apoptosis-inducing ligand receptor agonists in a xenograft model of Ewing's sarcoma. *Cancer Res* 2004; 64: 8349–8356.

27 Eliopoulos AG, Dawson CW, Mosialos G, Floettmann JE, Rowe M, Armitage RJ *et al*. CD40-induced growth inhibition in epithelial cells is mimicked by Epstein-Barr Virus-encoded LMP1: involvement of TRAF3 as a common mediator. *Oncogene* 1996; 13: 2243–2254.

28 Eliopoulos AG, Davies C, Knox PG, Gallagher NJ, Afford SC, Adams DH *et al*. CD40 induces apoptosis in carcinoma cells through activation of cytotoxic ligands of the tumor necrosis factor superfamily. *Mol Cell Biol* 2000; 20: 5503–5515.

29 Aaronson DS, Horvath CM. A road map for those who don't know JAK-STAT. *Science* 2002; 296: 1653–1655.

30 Choi EA, Lei H, Maron DJ, Wilson JM, Barsoum J, Fraker DL *et al*. Stat1-dependent induction of tumor necrosis factor-related apoptosis-inducing ligand and the cell-surface death signaling pathway by interferon beta in human cancer cells. *Cancer Res* 2003; 63: 5299–5307.

31 Griffith TS, Chin WA, Jackson GC, Lynch DH, Kubin MZ. Intracellular regulation of TRAIL-induced apoptosis in human melanoma cells. *J Immunol* 1998; 161: 2833–2840.

32 Miyasaki T, Reed JC. A GTP-binding adapter protein couples TRAIL receptors to apoptosis-inducing proteins. *Nat Immunol* 2001; 2: 493–500.

33 Nesterov A, Lu X, Johnson M, Miller GJ, Ivashchenko Y, Kraft AS. Elevated AKT activity protects the prostate cancer cell line LNCaP from TRAIL-induced apoptosis. *J Biol Chem* 2001; 276: 10767–10774.

34 Chen X, Thakkar H, Tyan F, Gim S, Robinson H, Lee C *et al*. Constitutively active Akt is an important regulator of TRAIL sensitivity in prostate cancer. *Oncogene* 2001; 20: 6073–6083.

35 Thakkar H, Chen X, Tyan F, Gim S, Robinson H, Lee C *et al*. Pro-survival function of Akt/protein kinase B in prostate cancer cells. Relationship with TRAIL resistance. *J Biol Chem* 2001; 276: 38361–38369.

36 Martelli AM, Tazzari PL, Tabellini G, Bortul R, Billi AM, Manzoli L *et al*. A new selective AKT pharmacological inhibitor reduces resistance to chemotherapeutic drugs, TRAIL, all-trans-retinoic acid, and ionizing radiation of human leukemia cells. *Leukemia* 2003; 17: 1794–1805.

37 Kikuchi T, Moore MA, Crystal RG. Dendritic cells modified to express CD40 ligand elicit therapeutic immunity against preexisting murine tumors. *Blood* 2000; 96: 91–99.

38 Kikuchi T, Miyazawa N, Moore MA, Crystal RG. Tumor regression induced by intratumor administration of adenovirus vector expressing CD40 ligand and naive dendritic cells. *Cancer Res* 2000; 60: 6391–6395.

39 Hemmings BA. Akt signaling: linking membrane events to life and death decisions. *Science* 1997; 275: 628–630.

40 Kennedy SG, Kandel ES, Cross TK, Hay N. Akt/Protein kinase B inhibits cell death by preventing the release of cytochrome c from mitochondria. *Mol Cell Biol* 1998; 19: 5800–5810.

41 Smyth MJ, Cretney E, Takeda K, Wiltrout RH, Sedger LM, Kayagaki N *et al*. Tumor necrosis factor-related apoptosis-inducing ligand (TRAIL) contributes to interferon gamma-dependent natural killer cell protection from tumor metastasis. *J Exp Med* 2001; 193: 661–670.

42 Miyazaki A, Sato N, Takahashi S, Sasaki A, Kohama G, Yamaguchi A *et al*. Cytotoxicity of histocompatibility leukocyte antigen-DR8-restricted CD4 killer T cells against human autologous squamous cell carcinoma. *Jpn J Cancer Res* 1997; 88: 191–197.

43 Nakamura T, Sato K, Hamada H. Effective gene transfer to human melanomas via integrin-targeted adenoviral vectors. *Hum Gene Ther* 2002; 13: 613–626.

44 Yoshida Y, Sadata A, Zhang W, Saito K, Shinoura N, Hamada H. Generation of fiber-mutant recombinant adenoviruses for gene therapy of malignant glioma. *Hum Gene Ther* 1998; 9: 2503–2515.

45 Kanegae Y, Lee G, Sato Y, Tanaka M, Nakai M, Sakaki T *et al*. Efficient gene activation in mammalian cells by using recombinant adenovirus expressing site-specific Cre recombinase. *Nucleic Acids Res* 1995; 23: 3816–3821.

46 Nyberg-Hoffman C, Shabram P, Li W, Giroux D, Aguilar-Cordova E. Sensitivity and reproducibility in adenoviral infectious titer determination. *Nat Med* 1997; 3: 808–811.

47 Uchida H, Tanaka T, Sasaki K, Kato K, Dehari H, Ito Y *et al*. Adenovirus-mediated transfer of siRNA against survivin induced apoptosis and attenuated tumor cell growth in vitro and in vivo. *Mol Ther* 2004; 10: 162–171.